Reversible Boron-Nitrogen Coordination in Organic Synthesis – From Bidentate Lewis Acid Catalysis to Materials

---

Inauguraldissertation zur Erlangung des Doktorgrades (Dr. rer. nat.) der
Naturwissenschaftlichen Fachbereiche im Fachgebiet Chemie der
Justus-Liebig-Universität Gießen

vorgelegt von

Julia Ruhl

aus
Nieder-Bessingen

Betreuer: Prof. Dr. Hermann A. Wegner

Gießen 2023

Versicherung nach §17 der Promotionsordnung

Ich erkläre: Ich habe die vorgelegte Dissertation selbstständig und ohne unerlaubte fremde Hilfe und nur mit den Hilfen angefertigt, die ich in der Dissertation angegeben habe. Alle Textstellen, die wörtlich oder sinngemäß aus veröffentlichten Schriften entnommen sind, und alle Angaben, die auf mündlichen Auskünften beruhen, sind als solche kenntlich gemacht. Ich stimme einer evtl. Überprüfung meiner Dissertation durch eine Antiplagiat-Software zu. Bei den von mir durchgeführten und in der Dissertation erwähnten Untersuchungen habe ich die Grundsätze guter wissenschaftlicher Praxis, wie sie in der „Satzung der Justus-Liebig-Universität Gießen zur Sicherung guter wissenschaftlicher Praxis“ niedergelegt sind, eingehalten.

Julia Ruhl Ort, Datum

Dekan:	Prof. Dr. Thomas Wilke
Erstgutachter:	Prof. Dr. Hermann A. Wegner
Zweitgutachter:	Prof. Dr. Richard Göttlich

„There's a child behind it, dreaming”

Alan Menken/Glenn Evan Slater

Table of Content

Abstract

The reversible coordination of the lone pair from a nitrogen atom into the free *p*-orbital of a boron atom can be used in various fields of organic synthesis and organic materials. This coordination is utilized in organic synthesis in the field of Lewis acid catalysis, for example in Friedel-Crafts and aza-Diels-Alder reactions, which clearly demonstrates its significance and applicability. This applicability was further extended in 2011 when the Wegner group employed the boron-based bidentate Lewis acid (BDLA), 9,10-dimethyl-9,10-dihydro-9,10-diboraanthracene, to show that the boron-nitrogen coordination can be used to catalyze inverse electron-demand Diels-Alder (IEDDA) reactions of phthalazines. By integrating the BDLA catalyzed IEDDA reaction into several domino processes, a diverse substrate scope with highly complex structures can be accessed. One of these domino processes combined an IEDDA reaction with a photoinduced ring-opening (PIRO) reaction of phthalazines with cyclic enamines and provided medium-sized carbocycles for the first time. These are core structures of many biologically active compounds and functional materials. Due to entropic and enthalpic reasons they cannot easily be synthesized and the synthesis normally requires transition-metal catalysis. Electron-rich as well as electron-poor phthalazines and cyclic enamines lead to various substituted 9- and 11-membered carbocycles in this BDLA catalyzed IEDDA/PIRO reaction (Figure 1).

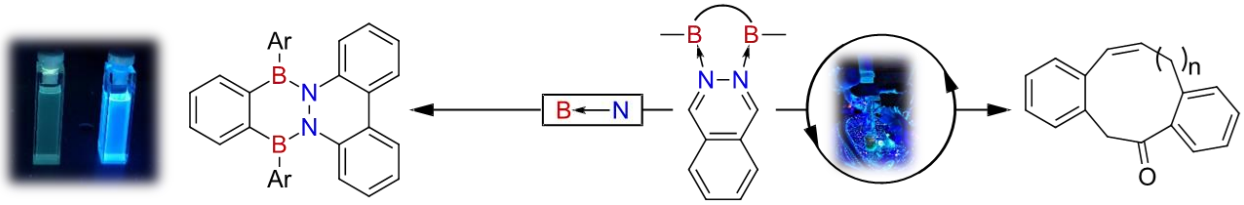

Figure 1: The reversible boron nitrogen coordination in Lewis acid catalysis and in synthesis of organic materials.

In the case of organic materials this coordination also has a major impact on boron-nitrogen doped polycyclic aromatic hydrocarbons (PAHs), e.g., in organic field-effect transistors (OFETs), organic light emitting diodes (OLEDs), or in solar cells. In 2017 the Wegner group published the synthesis of a stable boron-nitrogen doped biradical with a diazadiboraacene backbone. To access this novel diazadiborabenzo[*b*]triphenylenes and investigate their photophysical properties, a new modular synthetic strategy was developed. The investigation of the photophysical properties showed that even small changes of the substituent on the boron-atom lead to significant changes in the emission spectra.

Zusammenfassung

Die reversible Koordination des freien Elektronenpaars eines Stickstoffatoms in das freie *p*-Orbital eines Boratoms kann in verschiedenen Bereichen der organischen Synthese und für Materialien genutzt werden. Wie vielseitig diese Koordination in der organischen Synthese sein kann, zeigt sich in der Lewis-Säuren Katalyse, z. B. in Friedel-Crafts- und aza-Diels-Alder Reaktionen. Unter Verwendung der zweizähnigen Bor-Lewis-Säure, 9,10-Dimethyl-9,10-dihydro-9,10-diboraanthracen, zeigte die Wegner Gruppe in 2011, dass die Bor-Stickstoff-Koordination zur Katalyse von Diels-Alder Reaktionen mit inversem Elektronenbedarf (IEDDA) von Phthalazinen genutzt werden kann. Durch die Integration der Bor-Lewis-Säuren katalysierten IEDDA Reaktion mit verschiedenen Dominoprozessen konnten hochkomplexe Strukturen und eine vielfältige Substratbibliothek synthetisiert werden. Ein bereits etablierter Dominoprozess ist die Kombination der IEDDA Reaktion mit einer photoinduzierten Ringöffnungsreaktion (PIRO) von Phthalazinen und offenkettigen Enaminen. Um mit dieser Methode mittelgroße carbozyklische Verbindungen synthetisieren zu können, die den strukturellen Kern vieler biologisch aktiver Verbindungen und funktioneller Materialien bilden, wurden zyklische Enamine in dieser Methode etabliert. Diese carbozyklischen Verbindungen konnten aufgrund entropischer und enthalpischer Effekte bisher nur durch Übergangsmetallkatalyse synthetisiert werden. Unter Verwendung von elektronenreichen und elektronenarmen Phthalazinen und zyklischen Enaminen führt die Boran-katalysierte IEDDA/PIRO Reaktion zu einer Vielzahl unterschiedlich substituierten 9- und 11-gliedriger carbozyklische Verbindungen (Abbildung 1).

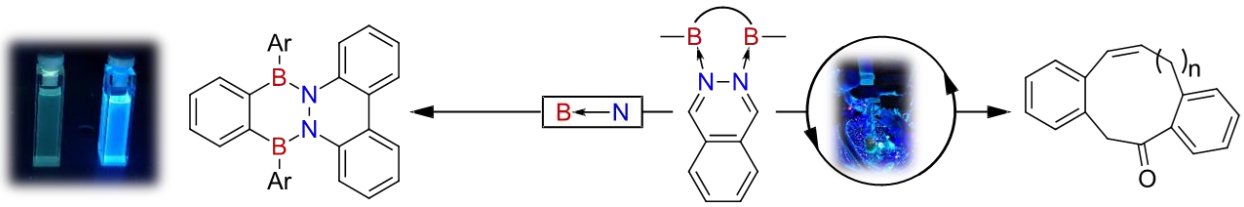

Abbildung 1: Die reversible Bor-Stickstoff Koordination in Lewis-Säuren-Katalyse und in der Synthese organischer Materialien.

Auch für organische Materialien ist die Bor-Stickstoff Koordination von großer Wichtigkeit. Die Bor-Stickstoff dotierten polyzyklischen aromatischen Kohlenwasserstoffen (PAHs), werden z.B. in organischen Feldeffekttransistoren (OFETs), organischen Leuchtdioden

(OLEDs) oder in Solarzellen genutzt. Im Jahr 2017 veröffentlichte die Wegner Gruppe die Synthese eines stabilen Bor-Stickstoff dotierten Biradikals, welches ein Diazadiboraacen-Grundgerüst besitzt. Um Zugang zu diesen neuartigen Diazadiborabenzo[*b*]triphenylenen zu erhalten und ihre photophysikalischen Eigenschaften zu untersuchen, wurde eine modulare Synthesestrategie entwickelt. Die Charakterisierung der photophysikalischen Eigenschaften zeigte, dass bereits kleine Änderungen der Substituenten am Bor-Atom zu signifikanten Änderungen in den Emissionsspektren führen.

1. Introduction

1.1. Boron-Nitrogen Coordination

Boron is part of the third main group of elements but its chemistry differs from the other elements in this group. Due to boron's unique electron configuration, it is capable of forming covalent bonds with both carbon and nitrogen.[1,2] As a result, boron plays a central role in organic chemistry and boron-containing compounds act as powerful tools for synthetic chemists. The two most popular examples for this are the Suzuki-coupling (A. Suzuki, Nobel prize 2010) and the hydroboration (H. C. Brown, Nobel prize 1979).[3] In contrast to the B-C bond, the boron-nitrogen single bond occurs from a coordination from the lone-pair of a nitrogen atom into the free *p*-orbital of a boron atom (Figure 2).

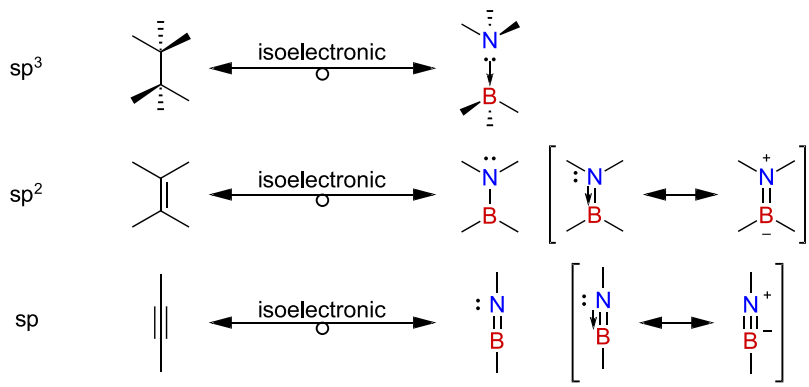

Figure 2: Isoelectronic relationship between C-C and B-N bonds.[1]

The boron-nitrogen coordination enables the formation of bonds which are equal to different hybridized C-C bonds in their steric and electronic properties. This comparison shows that bonds are isosteric and isoelectronic to each other, due to their identical valence electron count (B-N bond: B $3e^-$, N $5e^-$ and C=C bond: each C $4e^-$), but their chemical and physical properties are significantly different. One of the simplest examples to use to demonstrate this relationship is ethane and ammonia borane. Ethane is a gas under standard conditions with a boiling point of −89 °C.[4] It has no effective dipole moment and the bond dissociation energy (BDE) of the C-C bond is 90.1 kcal · mol^{-1}.[5] In contrast to that, ammonia borane is a solid under standard conditions with a melting point of 104 °C.[6] It has a strong dipole moment (5.2 Da) and the BDE is 27.1 kcal · mol^{-1}.[1,7] It is however important to note that the BN/CC isomerism could also be apply to arenes.

One of the most popular examples for BN/CC isosterism is borazine (**1**). It is the inorganic counterpart to the quintessential aromatic compound benzene. Additionally, borazine (**1**) was the first example of BN/CC isosterism of an arene when it was reported by Alfred Stock in 1926 (Figure 3).[8]

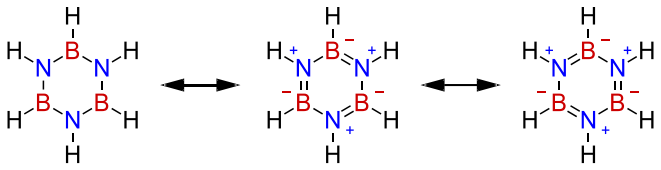

1

Figure 3: Mesomeric structures of borazine (**1**).

1.2. The Boron-Nitrogen Coordination in Lewis Acid Catalysis

Apart from their extraordinary structural interactions, the coordination of the lone pair of a nitrogen atom into the free *p*-orbital of a boron atom has proven instrumental in Lewis acid catalysis, e.g. in Friedel-Crafts and aza-Diels-Alder reactions.[9,10] The first example, that was reported, was the Diels-Alder (DA) reaction, the parent carbon based equivalent to the aza-DA, in the addition of isoprene and 1,4-benzoquinone by H. v. Euler and K. O. Josephson in 1920.[11] Nevertheless, this reaction was ultimately named after O. Diels and K. Alder, who investigated the mechanism of the [4+2] cycloaddition with six π-electrons for the reaction between cyclopentadiene and 1,4-benzoquinone in 1928.[12] In 1950, O. Diels and K. Alder received the Nobel prize in chemistry for their work on this topic and their contribution to the understanding of these kind of reactions.[13] Since then, the DA reaction has been established as one of the most utilized reaction types as it offers the great advantage of installing potentially four stereocenters in one step.[13] In the shadow of the DA reaction, the inverse electron-demand Diels-Alder (IEDDA) reaction has slowly gained interest over the past decades.[14]

As mentioned above the DA reaction is a [4+2] cycloaddition. Four of six π-electrons must be located on the conjugated diene and two on the dienophile. The conjugated diene can be cyclic or non-cyclic. To simplify the mechanism of the DA reaction, it is often shown by the example reaction of butadiene (**2**) and ethene (**3**) as illustrated in Scheme 1. The butadiene (**2**) reacts with ethene (**3**) under the selective formation of two σ-bonds and one π-bond during a pericyclic, concerted transition state to form cyclohexene (**4**). Hence, the

DA reaction can be used as highly efficient construction reaction with perfect atom economy.[15]

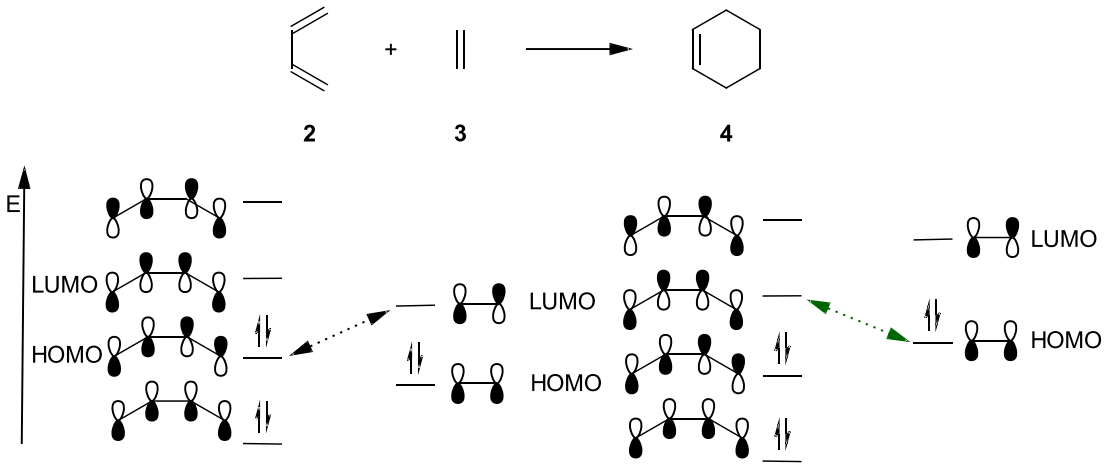

Scheme 1: Molecular orbital diagram of the Diels-Alder (DA) reaction (black - left) and the inverse electron demand Diels-Alder (IEDDA) reaction (green - right).

In a DA reaction the highest occupied molecular orbital (HOMO) of the diene and the lowest unoccupied molecular orbital (LUMO) of the dienophile react with each other.[13] However, by altering the substituents on the diene and the dienophile it is also possible that the LUMO of the diene and the HOMO of the dienophile can react with each other. This reaction is known as the IEDDA reaction.[15,16] Whether the diene and the dienophile react in a DA or in an IEDDA reaction is dependent on the more favourable orbital interactions. It is known that, the DA reaction can be favoured by incorporating electron donating groups (EDG) on the diene and electron withdrawing groups (EWG) on the dienophile. The EDG on the diene lifts the HOMO of the diene energetically and the EWG on the dienophile lowers the LUMO of the dienophile in energy. As a result, the gap between the HOMO and LUMO becomes smaller. The same principle is valid in the opposite direction for the IEDDA reaction.[13,15]

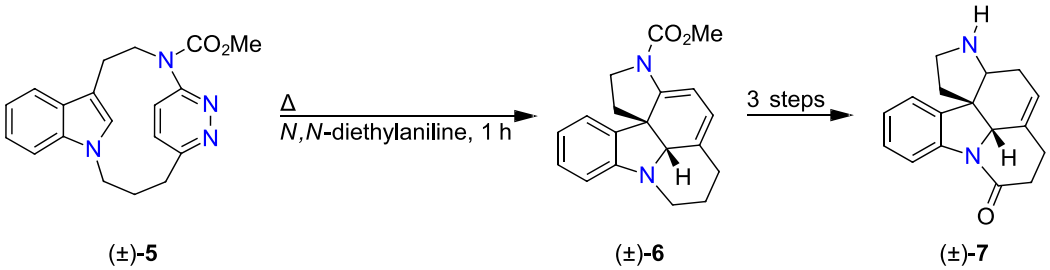

Scheme 2: IEDDA reaction in the total synthesis of strychnine (**7**).[14]

One example to show what a powerful tool the IEDDA reaction can be was reported by Graham J. Bodwell and Jiang Li in 2002 (Scheme 2).[14] In the total synthesis of strychnine (**7**), they used the IEDDA reaction as key step to form the pentacycle **6** in a stereospecific way. This example does, however, also demonstrated, that IEDDA reactions with compounds containing diazine-units, have to normally be performed under harsh conditions.[14,17] With increasing number of nitrogen-atoms in the diene cores, e.g., when using triazines or tetrazines, the electron-deficient character of the diene is increased. This leads to an energetically lowered LUMO of the diene which subsequently provides a higher reactivity.[18] Dale L. Boger and co-workers used these electron-deficient dienes in the aza-IEDDA reaction as key-steps in various total synthesis of natural products, e.g., streptonigrin (1983),[19] (-)-pyrimidoblamicc acid (1993),[20] (-)-vindoline (2006 and 2015),[21] and methoxatin (2016).[22] Activation problems can occur in certain DA or IEDDA reactions, as in the total synthesis of strychnine (**7**), but this can be overcome by making use of Lewis acid (LA) catalysis. The coordinated LA, e.g. BF_3, can lower the LUMO of the diene (IEDDA) or dienophile (DA) energetically thereby reducing the HOMO-LUMO gap making it possible to use more lenient conditions.[15]

1.2.1. Monodentate Boron-Based Lewis Acid Catalysis of IEDDA reactions

One of the first examples of boron-based Lewis acid catalysis in IEDDA reactions with aza-dienes was shown by Povarov and Mikhailov in 1964.[23] They formed the Schiff base **8** *in situ* by using aniline and an excess of the vinyl ethyl ether **9** (Scheme 3). Under LA catalysis with BF_3 the dienophile **9** can react with the aza-diene **8** in the IEDDA reaction, and after re-aromatization, the tetrahydroquinoline **10** is obtained in a yield of 30%.

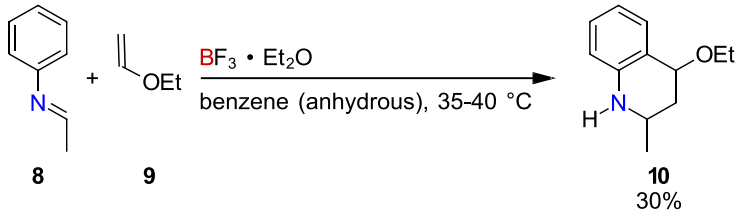

Scheme 3: IEDDA reaction of the Schiff base **8** and vinyl ethyl ether **9** catalyzed with $BF_3 \cdot Et_2O$.[23]

In 1985 Cheng *et al.* showed that the IEDDA reaction of aza-dienes with electron-rich dienophiles is also possible in the present of the strong LA $BF_3 \cdot Et_2O$ as catalyst.[10] Beforehand, this kind of compounds could only react with electron-poor dienophiles, like

maleic anhydride, or at temperatures above 200 °C in a DA reaction.[24] Within this publication they showed the BF_3 catalyzed IEDDA reaction of the aza-diene **11** with 1-morpholinocyclopentene (**12**) as dienophile. The coordination of the nitrogen of the aza-diene **11** to the boron of the BF_3 leads to a lowering in energy of the LUMO of the aza-diene **11** so that the IEDDA reaction can proceed at 25 °C. By reducing the BF_3-tetrahydropyridine complex **13** with sodium boron hydride the corresponding 1-phenyl-4-methyl-9-morpholino-2-azaindans **14** and **15** were obtained in an overall yield of 39% (Scheme 4).

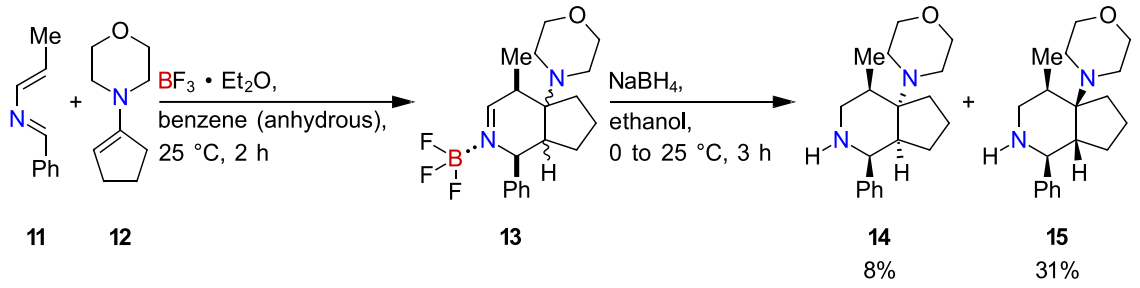

Scheme 4: BF_3 catalyzed IEDDA reaction of aza-diene **11** and 1-morpholinocyclopentene (**12**).[10]

Nevertheless, when compounds with a larger number of nitrogen atoms, like 1,2-diazines or 1,2,3,4-tetrazines, are employed in the IEDDA reaction the monodentate Lewis acid catalysts can only coordinate to one site of the substrate. In these cases, a bidentate Lewis acid catalyst, which can coordinate to two conjugated nitrogen atoms, should lead to a more significant drop in energy of the LUMO of the electron-rich diene. With this in mind, several examples of bidentate Lewis acid catalysts, including aluminum and titanium based systems, were synthesized. Unfortunately, nearly all of them only form one bond/coordination with the substrate.[25] On the other hand, there has been several boron-based Lewis acids reported, which are binding in the bidentate manner to 1,2-dinitrogen compounds, e.g. 1,2-diazines, but they were never used in this context.[26–28]

1.2.2. Bidentate Boron-Based Lewis Acid Catalysis of IEDDA reactions with Phthalazines (24)

Based on the studies of boron-based anthracene structures[26,29,30] and the indium-based bidentate Lewis acid-phthalazine-complex **17**,[28] which are selective to 1,2-diazines, the Wegner group designed 9,10-dimethyl-9,10-dihydro-9,10-diboraantharacene (**21**) as catalyst in the IEDDA reaction of 1,2-diazines.[31] In Figure 4 the similarities of the crystal

structure of the boron-based as well as the indium-based Lewis acid-phthalazine-complexes **16** & **17** are depicted.[28,32] Both Lewis acids form a triptycene-like structure by coordination with the phthalazine (**24**).

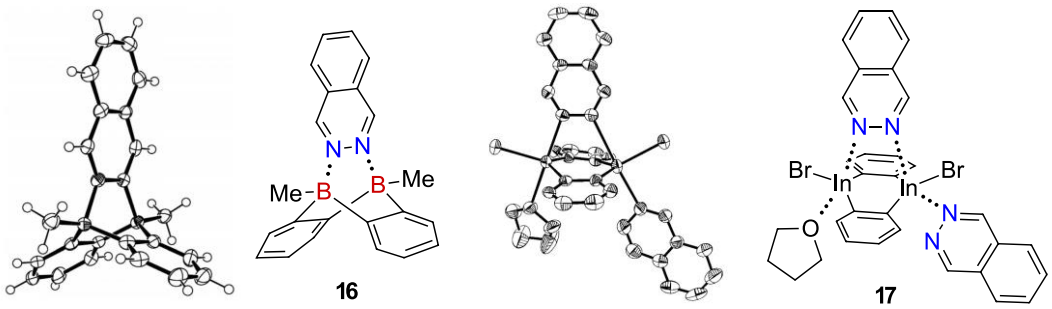

Figure 4: ORTEP drawing (50% probability) and skeletal formula of the boron-based bidentate Lewis acid/phthalazine complex **16** (left) and indium-based Lewis acid/phthalazine complex **17** (right).[28,32]

The synthesis of 9,10-dimethyl-9,10-dihydro-9,10-diboraanthracene (**21**) was reported by Schulz *et al.* in 1991.[29] In their four-step procedure, they obtain **21** in an overall yield of less than 5%. To gain better access to the 9,10-dimethyl-9,10-dihydro-9,10-diboraanthracene (**21**), the synthesis was significantly improved in the last decades. In 2010 Bader *et al.* showed a new three-step synthesis of **21** with an overall yield of 27% (Scheme 5).[33]

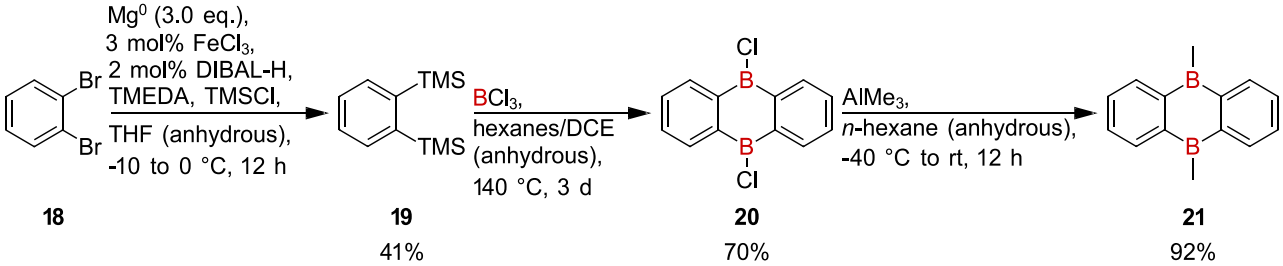

Scheme 5: Synthetic route for 9,10-dimethyl-9,10-dihydro-9,10-diboraanthracene (**21**).[33]

The synthesis of the boron-based bidentate Lewis acid **21** started with an iron-catalyzed Grignard reaction of 1,2-dibromobenzene (**18**) to obtain 1,2-bis(TMS)aryl compound **19** in a moderate yield. This step can even be performed on a multigram scale and with different substituents.[32,33] An alternative route for this transformation by a magnesium Grignard reaction without iron catalyst was later published.[34] The dimer **20** is subsequently formed by stirring **19** and BCl_3 in anhydrous DCE in a sealed pressure tube at high temperatures for three days. Upon cooling the air- and moisture-sensitive product crystallizes as white needles. The solvent was removed, and the needles were washed with hexanes.

Following this procedure, the dimer was obtained in good yields. In the final step, the chlorine on the boron was exchanged to a methyl group by $AlMe_3$.[33]

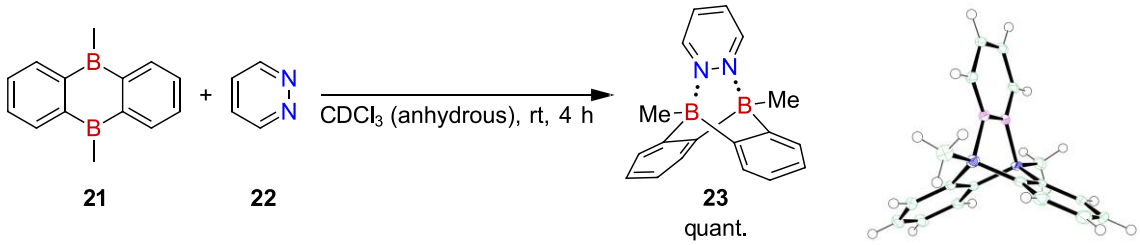

Scheme 6: Synthesis of the air-stable pyridazine/Lewis acid complex **23** (left). ORTEP drawing (50% probability) of complex **23** (right).[35]

The preparation as well as the handling of **21** is only possible under Schlenk conditions. To overcome this disadvantage, Hong *et al.* showed the synthesis of an air and moisture stable catalyst variant **23** in 2018.[35] The Wegner group demonstrated that the catalyst **21** can be synthesized in a one-pot reaction starting form 1,2-bis(TMS)aryl compound **19** with BBr_3 and $AlMe_3$ in a yield of 51%. Additionally, it was shown that the air and moisture sensitive Lewis acid **21** could be quantitatively converted with pyridazine (**22**) to the triptycen like air-stable complex **23** (Scheme 6).[35]

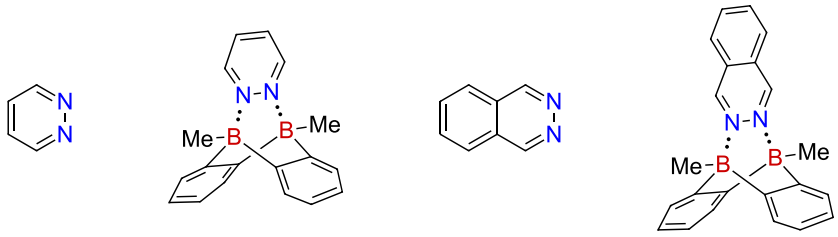

	22	23	24	16
LUMO	0.44	-3.16	-1.76	-3.05
HOMO	-2.98	-5.32	-6.34	-5.15

Figure 5: FMO energies in eV of the HOMO and the LUMO of pyridazine (**22**), phthalazine (**24**), and their complexes with Lewis acid **21**, [computed on B3LYP/6-31g(d,p) level of theory].[36]

The pyridazine (**22**) leads to a tetra-coordination of the boron atoms. The free *p*-orbital of the boron is thereby blocked, and stabilizes the complex **23** towards oxidation and hydrolysis. In solution the coordination of the nitrogen to the boron is reversible, which makes complex **23** useful in a variety of IEDDA reactions and allows the coordination of other 1,2-diazine moieties to the BDLA **21**.[36] Besides the stabilization effect, complex **23** also has the benefit that the LUMO level of pyridazine (**22**) is significantly lowered by complexation. This is similar for phthalazine (**24**) which can also coordinate as 1,2-diazine

to the boron-atoms in catalyst **21**. This leads to smaller HOMO-LUMO gap between the diazines **22** & **24** and electron-rich dienophiles, and IEDDA reactions can proceed under milder conditions. DFT computations were carried out on B3LYP/6-31g(d,p) level of theory (Figure 5).[36,37] However, pyridazine (**22**) is not reacting in this BDLA-catalyzed IEDDA reaction with electron-rich dienophiles **25** due to a loss of aromaticity during the initial cycloaddition. In contrast to that, when using phthalazine (**24**) only the aromaticity of one ring is broken during the reaction (Scheme 7).[32]

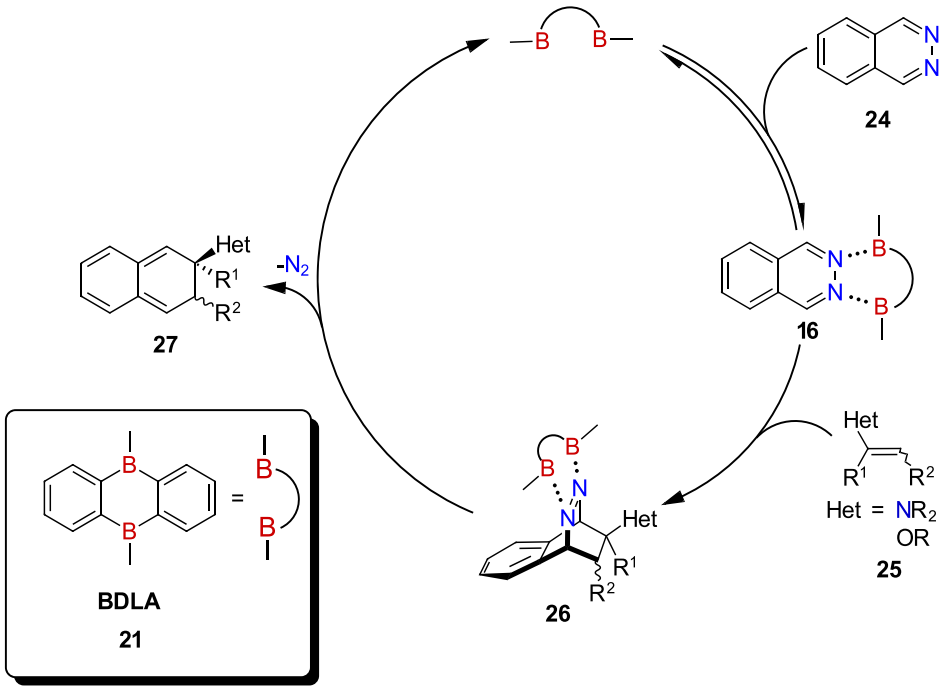

Scheme 7: Catalytic cycle of BDLA **21** participating in an IEDDA reaction of phthalazine (**24**) and a dienophile **25** to form the highly reactive intermediate **27**.[38–41]

The coordination of the 1,2-diazine moiety of the phthalazine (**24**) to the boron-based bidentate Lewis acid **21** (BDLA) and the resulting energetically lowered LUMO of the diazine, was intensively investigated in Lewis acid catalyzed IEDDA reactions with phthalazines (**24**) with electron-rich dienophiles **25** in the Wegner group.[39,40] In the first step of the catalytic cycle, the BDLA **21** coordinates to the phthalazine (**24**) to form the diazine/Lewis acid complex **16**. As for the air-stable catalyst **23** the formation of this complex **16** is also a reversible process in solution. Then, the complex **16** reacts in an IEDDA reaction with the electron-rich dienophile **25** to the IEDDA product **26**. Under the split-off of the BDLA **21** and N_2 elimination a highly reactive *o*-quinodimethane intermediate **27** is formed. This intermediate **27** can then undergo a large variety of

subsequent reactions.[32] The type of product depends on the reaction conditions and the substitution of the chosen dienophile (Scheme 8).[31,32,38–46]

Furthermore, also starting from the intermediate **27**, naphthalene derivatives **28** can be formed by elimination reactions.[31] For example, if an enamine with a second double bond is used as dienophile for the IEDDA reaction, highly complex molecules like **31** and **32** can be formed during a following DA reaction.[39] When using an excess of amines or thiophenols, an asymmetric rearrangement is observed, which leads to structures like **33**.[42,43] The main driving force for all these subsequent reactions is re-aromatisation of the *o*-quinodimethane intermediate **27**.[31,32,38–46] Besides temperature and concentration of the reagents, an additional parameter, which is sometimes forgotten, but especially efficient in pericyclic reactions, is light. In this case, the irradiation of *o*-quinodimethane intermediate **27** with a blue LED enables a photoinduced ring-opening (PIRO) reaction.

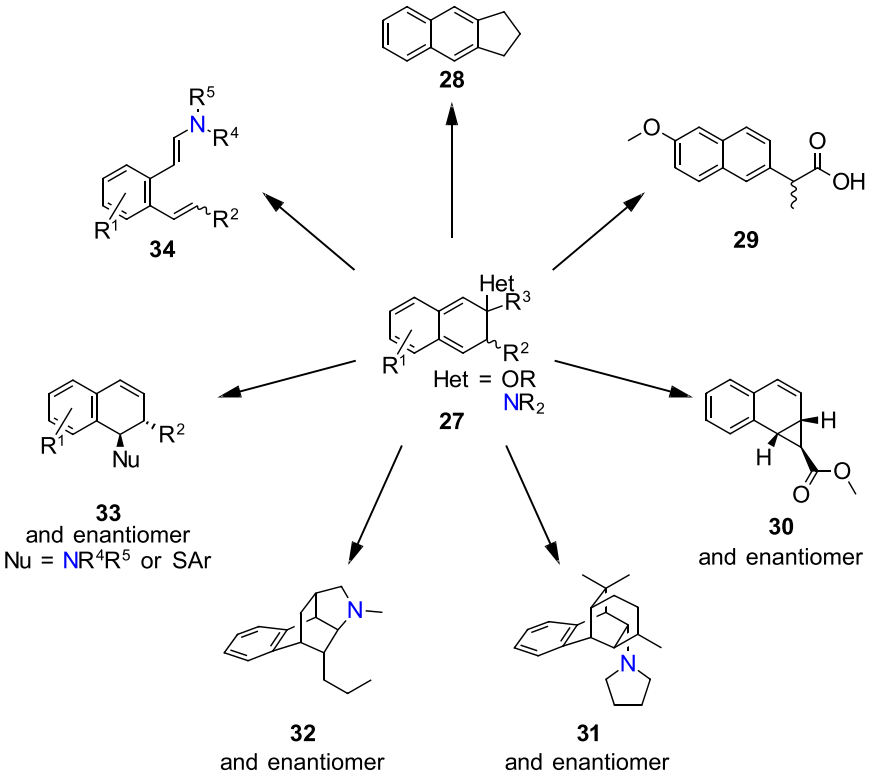

Scheme 8: Possible products of the BDLA catalyzed IEDDA reaction with phthalazine (**24**) depending on dienophiles and reaction conditions.[31,32,38–46]

This pericyclic PIRO reaction of the *o*-quinodimethane intermediate **27** proceeds according to the Woodward-Hoffmann rules with its 10π-electron in conrotatory fashion to form product **34**. For improved purification the enamine **34** was reduced with $NaBH(OAc)_3$

and AcOH in DCM to its corresponding more stable phenethylamine **35** in a yield of 81%. Several other amines, phthalazines and aldehydes were used in the IEDDA/PIRO reaction. Depending on the irradiation wavelength, reaction temperature and substitution scaffold, the corresponding amines were obtained in moderate to good yields (Scheme 9).[41]

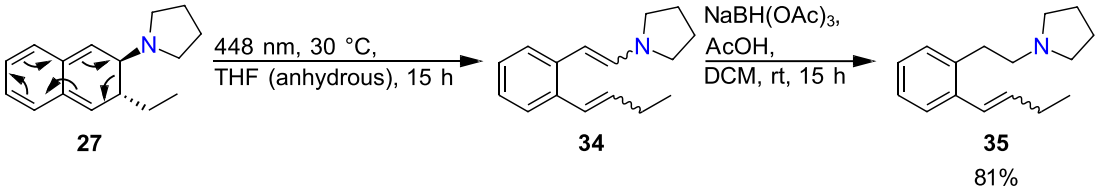

Scheme 9: PIRO reaction of the *o*-quinodimethane intermediate **27** and following reduction with $NaBH(OAc)_3$ and AcOH in DCM to the corresponding amine **35**.[41]

1.3. Boron-Nitrogen Doped Polycyclic Aromatic Compounds

The usage of reversible boron-nitrogen coordination is not limited to Lewis acid catalysis. The coordination also has a huge impact in boron-nitrogen doped polycyclic aromatic hydrocarbons (PAHs). PAHs have received attention in materials research due to their application potential, e.g. in organic field-effect transistors (OFETs),[47] organic light emitting diodes (OLEDs),[48] as well as in solar cells.[49] This is related to their versatile structure dependent properties which is accessible through their modular synthesis.[50] Additionally, the implementation of boron atoms in PAHs was shown to lead to new exceptional optoelectronic materials.[1,51] As mentioned above the valence electron count of a B-N and of a C=C bond is the same (BN/CC isosterism). Therefore, C=C bonds can be replaced by B-N bonds.[1] Because of the difference in electronegativity of boron and nitrogen, a dipole moment is introduced in the PAH, which can significantly influence the solid-state structure as well as electronic and optoelectronic properties, while maintaining the existing molecular structural features. These changes are due to the modification of the HOMO-LUMO gap as well as the intermolecular interactions in the solid state.[1,2,52]

1.3.1. Separated B-N Bonds in PAHs

Pioneers in the field of azaboraacences synthesis were Dewar and co-workers in the 1950s and 1960s. One of their first publications on azaboraacences was the synthesis of azaboranaphthalene derivatives **37-42** in 1959 (Scheme 10).[53] They published a synthesis in which 2-aminostyrene (**36**) was reacted with boron trichloride to obtain

2-chloro-2,1-borazaronaphthalene (**37**). Starting from the 2-chloro-2,1-borazaronaphthalene (**37**), the synthesis can be varied and multiple different derivatives can be prepared. After the reaction with lithium aluminium hydride, the 2,1-borazaronaphthalene (**38**) is generated, with water bis-2,1-borazaro-2-naphthyl ether (**41**) is yielded. In Grignard reactions of 2-chloro-2,1-borazaronaphthalene (**37**), with methyl iodide 2-methyl-2,1-borazaronaphthalene (**42**) is obtained and with bromobenzene, 2-phenyl-2,1-borazaronaphthalene (**40**) is formed. The latter can also be synthesized directly from 2-aminostyrene (**36**) with phenyl boron dichloride (**39**).[53–55]

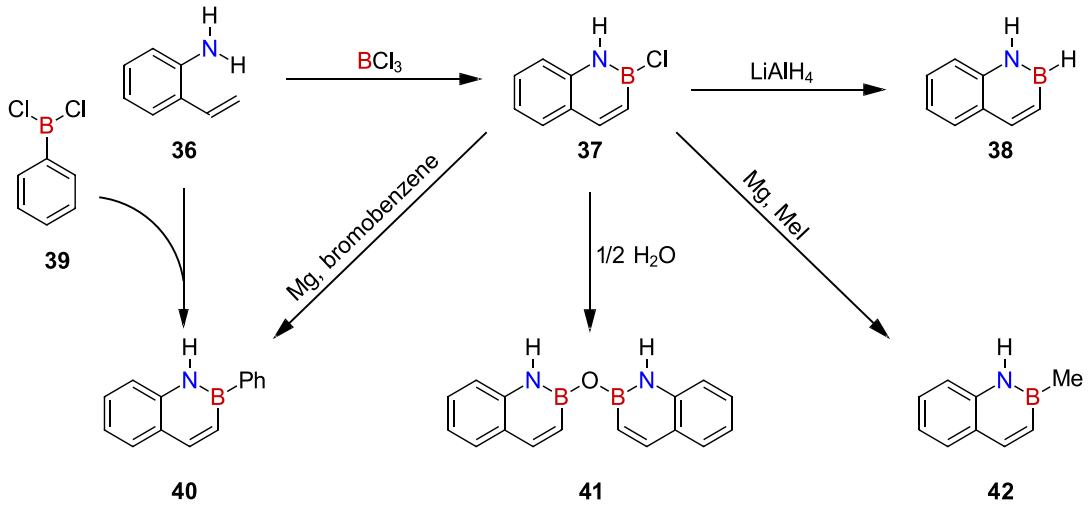

Scheme 10: Synthesis of azaboranaphthalenes **37-42** by Dewar in 1959.[53]

Nonetheless, they did not only replace one C=C bond with a B-N bond in polyaromatic systems. Shortly afterwards they showed the synthesis of the azaboranaphthalenes **37-42**, they published the synthesis of diazadiborapyrene **44** and diazadiboraantharacene **46**.[56] The diazadiborapyrene **44** was formed by heating [1,1′-biphenyl]-2,6-diamine (**43**) with phenylboron dichloride and was obtained in a yield of 21%. In a similar fashion, the diazadiboraantharacene **46** was synthesized from the corresponding diamine **45** in an excellent yield of 94%.

Additionally, they started to investigate the optoelectronic properties of their boron-nitrogen doped PAHs.[57] After Dewar and co-workers pioneering work, new methods for the preparation of existing and new BN isosters of PAHs have been developed.[58,59] For example, regarding the tricyclic BN isosters of PAHs, following on Dewar's work, Williams

and co-workers developed the oxidative photocyclization of aniline boranes to obtain 9,10-azaboraphenanthrenes.[60]

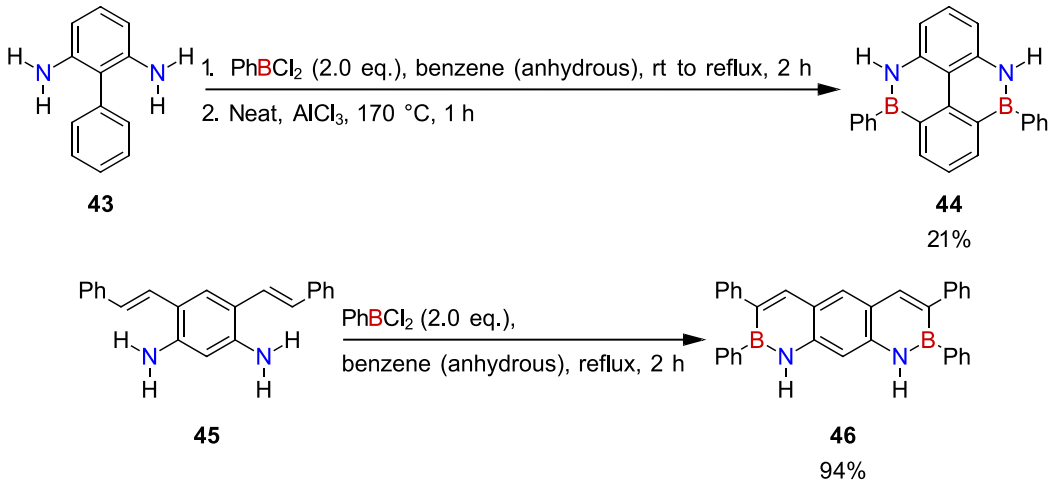

Scheme 11: Synthesis of the diazadiboraacences **44** and **46** from their corresponding starting materials with phenylboron dichloride.[56]

More recently, in 2007 Piers and co-workers prepared “internal” azaboraphenanthrene isosteres 4a,4b-azaboraphenanthrene **50a-d**.[61] They used 1-chloro-trimethylsilyl-boracyclohexa-2,5-diene (**47**) and a variety of 2-ethynyl-pyridines **48a-d** as starting materials. Under the elimination of TMSCl the borabenzene-pyridine adducts **49a-d** were formed first. By stirring the reaction mixture for an additional 36 hours at room temperature, azaboraphenanthrenes **50a-c** could be isolated in moderate to excellent yields after cycloisomerization. In the equivalent all-carbon system, this kind of reaction requires transition metal catalysis.[62] Due to slow cycloisomerization at 25 °C **49d** could be isolated. This decrease in reactivity is likely an effect of the reduced electrophilicity of the terminal carbon atom of the alkyne moiety due to the electropositive nature of the connected silicon atom. The cycloisomerization of **49d** proceeds by heating the reaction mixture at 80 °C for 24 h to afford **50d** in a yield of 79% over two steps (Scheme 12).[61]

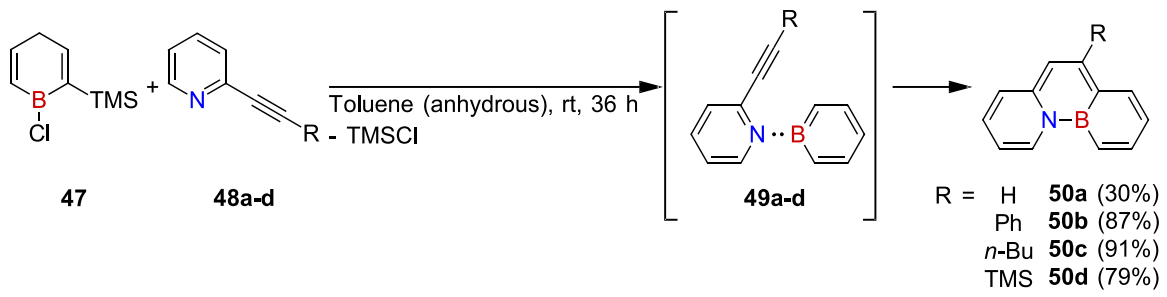

Scheme 12: Synthesis of "internal" azaboraphenanthrene isosterse 4a,4b-azaboraphenanthrene **50a-d**.[61]

In this study, they also synthesized, in a modified approach to Dewar's work,[54] azaboraphenanthrene derivatives with an "external" B-N bond, e.g. **51**. With this, they had the possibility to directly compare the photophysical properties of the "internal" and "external" B-N bond in a phenanthrene scaffold, and the all-carbon phenanthrene (**52**) with each other (Figure 6).

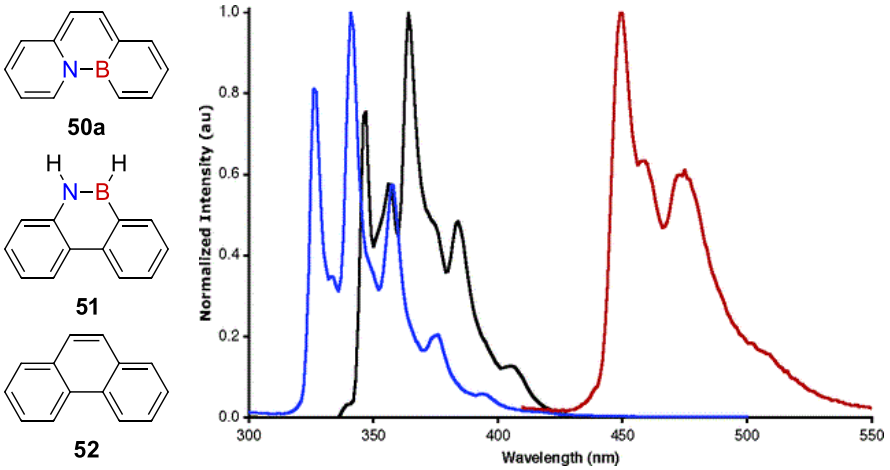

Figure 6: Fluorescence spectra of phenanthrene (**52** - black line, $\lambda_{ex.}$ = 260 nm), 9,10-BN phenanthrene **51** (blue line, $\lambda_{ex.}$ = 330 nm), and 4a,4b-azaboraphenanthrene **50a** (red line, $\lambda_{ex.}$ = 330 nm) in cyclohexane.[61]

In this case, phenanthrene (**52**) ($\lambda_{ex.}$ = 260 nm) which is a well-known fluorophore with an emission wavelength of $\lambda_{em.}$ = 347 nm and a quantum yield of Φ_F = 0.09 was used as reference.[63] In comparison with phenathrene (**52**) the emission of the 4a,4b-azaboraphenanthrene **50a** ($\lambda_{ex.}$ = 330 nm) is red-shifted and has an emission maximum at 450 nm and a quantum yield of Φ_F = 0.58, observable as a bright blue light emission. The Stokes shift of **50a** ($\lambda_{ex.}$ = 330 nm) which is 4 nm ($\lambda_{abs..}$ = 446 nm) is relatively small in comparison to phenanthrene (**52**), which has a Stokes shift of 54 nm ($\lambda_{abs..}$ = 293 nm). With an absorption maximum of 326 nm and an emission maximum of 327 nm, the 9,10-azaboraphenanthrene **51** shows an even smaller Stokes shift (1 nm) than **50a**.

Additionally, the emission of **51** is more similar to the phenanthrene (**52**) with only a marginal blue shift. Due to the central position of the B-N moiety in 4a,4b-azaboraphenanthrene **50a**, a local dipole moment is introduced into the core structure, and with this into the fluorogenic unit. This is influencing the molecular properties drastically. In contrast to this, in the 9,10-azaboraphenanthrene **51** the B-N moiety has an external position and acts more as a bridge and is not polarizing the fluorophore.[61] This shows how important the position of the B-N moiety in PAHs is to influence the electronical properties.

In the same year, Piers and co-workers published the synthesis of central substituted B,N pyrenes **56a-c**.[58] They used a similar synthetic route as for 4a,4b-azaboraphenanthrenes **50a-c**. In the first step, the pyridines **53a-c** coordinate to 1-chloro-trimethylsilyl-boracyclohexa-2,5-diene (**47**) and under elimination of TMSCl, borabenzene-pyridine adducts **54a-c** are formed. The azaboraphenanthrenes **55a-c** are obtained by a cycloisomerization reaction of one of the alkyne groups. For the second cyclization, the distance between the terminal carbon atom of the remaining alkyne group and the carbon in *α*-position to the boron in the more rigid azaboraphenanthrenes **55a-c** (3.5 Å) is larger than in adducts **54a-c** (2.9 Å). Consequently, the cyclization has to be catalyzed with 5 mol% of $PtCl_2$ at 90-95 °C (Scheme 13). Because of their π-stabilized structure, the BN pyrenes **56a-c** are air- and moisture-stable and can be obtained in moderate to very good yields after column chromatography. In general, there are two possible strategies to stabilize a trivalent boron in PAHs. One is stabilization by embedding it into the inner part of PAHs, like in this case. This is called “principle of structure constraint”. Herein, the tetra coordinated adducts of the boron become unfavourable and C−B bond cleavage is prevented by the chelating effect.[64] The second possibility is the use of bulky substituents (e.g. mesityl-groups) on the boron, which blocks the free *p*-orbital of the boron and leads to kinetic protection. This is called “principle of steric shielding”.[65]

Additionally, Piers and co-workers investigated the photophysical properties of the BN pyrenes **56a-c** in comparison to the all-carbon pyrene. Herein, it was shown that the polarization of the pyrene moiety leads to a red-shift in the emission spectra ($\lambda_{ex.,\mathbf{56a\text{-}c}}$ = 330 nm; $\lambda_{ex.,pyrene}$ = 337 nm; $\lambda_{em,\mathbf{56a\text{-}c}}$ = 488 – 489 nm, $\lambda_{em,pyrene}$ = 383 nm; both in cyclohexane)[66] to a visible green fluorescence of **56a-c**, but the quantum yields are much

lower than for the pyrene ($\Phi_{F,pyrene}$ = 0.60, $\Phi_{F,\mathbf{56a\text{-}c}}$ = 0.11 – 0.16; both in cyclohexane). Nevertheless, in photophysical studies with **56a-c**, they showed that excimer behaviour of the pyrene is also observed in azaborapyrene **56a-c** and the fluorescence can even be shifted to 510 – 550 nm ($\lambda_{em.,excimer\ pyrene}$ = 470 nm).[58]

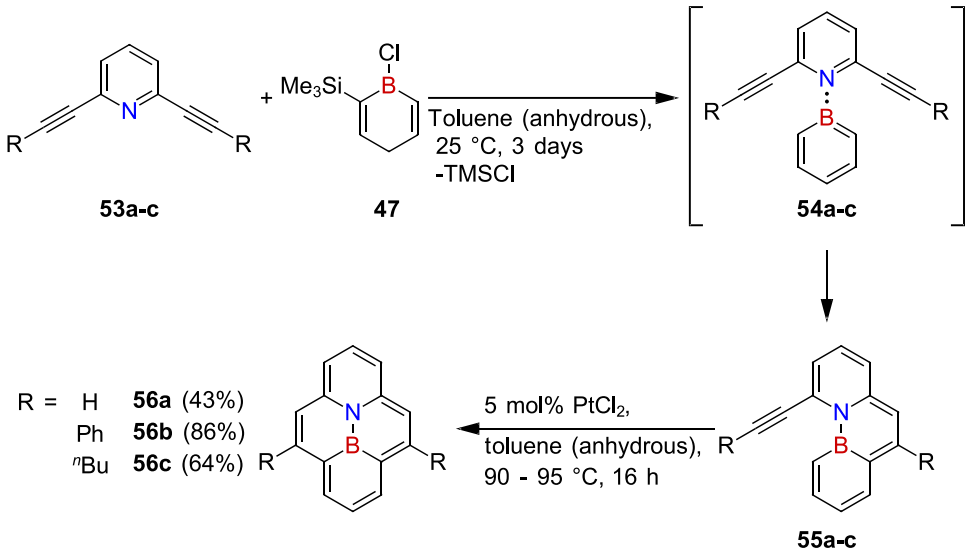

Scheme 13: Synthesis of 10a,10b-azaborapyrenes **56a-c**.[58]

This selection of B,N-PAHs with separated B-N bonds was specifically chosen to show the development of this field, starting from the B,N-PAHs by Dewar and co-workers up until the investigations done by Piers and co-workers, which proved how important the position of the B-N bonds are. Piers and co-workers could specifically show that the implementation of B-N bonds into the core structure has a significant impact on the molecule properties. To increase this effect even further, the dipole moment in the core structure would have to be enhanced. This could be achieved by introducing connected B-N-N-B bonds in a core position of PAHs.

1.3.2. Connected B-N Bonds in PAHs

The first example of diazadiboraacene, in which the two B-N bonds are connected via an N-N bond, was shown by Siebert and co-workers in 1974.[67] Starting from 1,3-dimethyl-2,1,3-benzothiadiborolane (**57**), they showed the conversion with aniline and methylamine under the elimination of H_2S to the corresponding azadiboraacences (B-N-B connected). Additionally, in the same reaction set-up with hydrazine they were able to form the diazadiboranaphthalene (**58**). After distillation, **58** was obtained in a good yield of 70%

(Scheme 14).[67,68] Later on, they were able to show that this reaction could be performed with methylhydrazine and *N,N'*-dimethylhydrazine to afford the corresponding diazadiboranaphthalenes.[69,70]

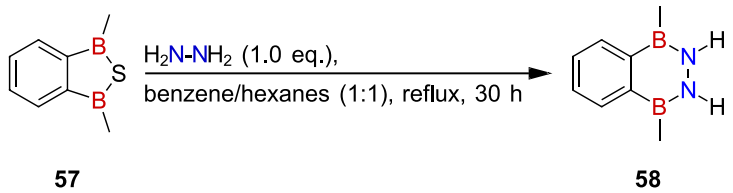

Scheme 14: Synthesis of diazadibornaphthalenes **58** from thiaborolene **57** with hydrazine by Siebert and co-workers in 1974.[67–70]

It took nearly 30 years until the synthesis of new diazadiboraacence derivatives was published. Finally in 2003, Piers and co-workers showed the synthesis of diazadiboratriphenylene **64a**.[71]

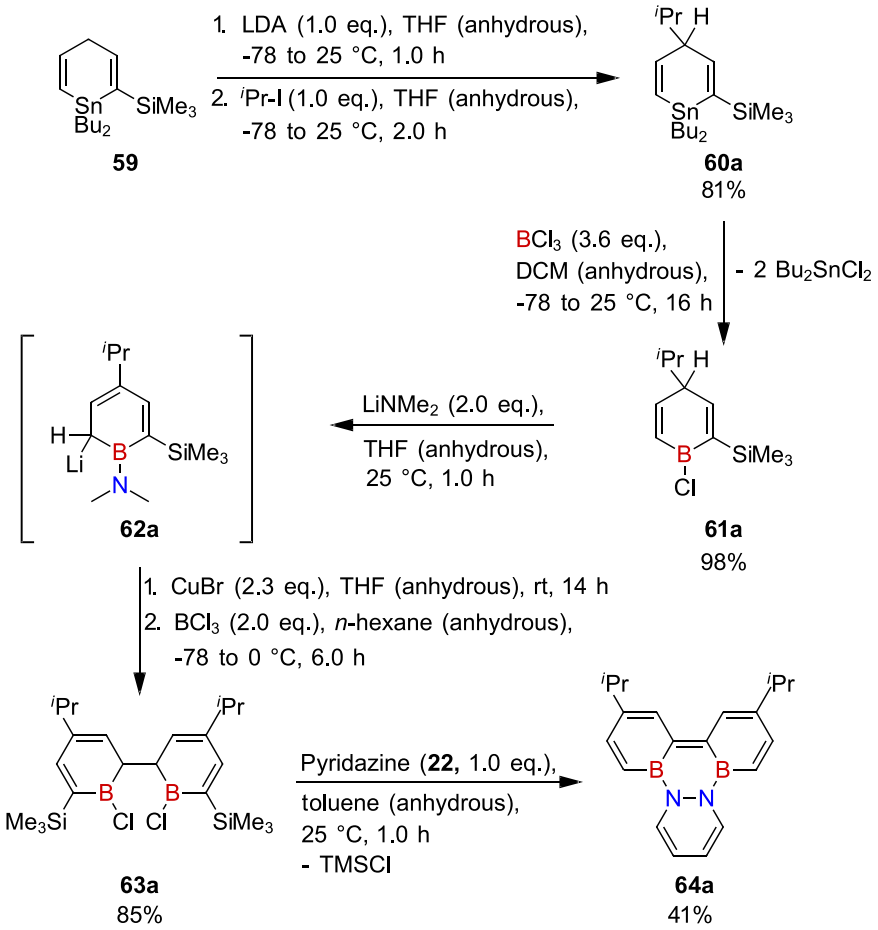

Scheme 15: Synthesis of the diazadiboratriphenylene **64a** starting from stannacyclohexadiene **59**.[71]

To receive the boron dimer **63a** starting from stannacyclohexadiene **59**, the crucial C-C bond-forming step has to proceed selectively in *ortho*-position to the boron atom. Therefore, it was necessary to first block the *para*-position. Firstly, the stannacyclohexadiene **59** was deprotonated with LDA followed by quenching of the lithium salt with isopropyl iodide. Due to the high regioselectivity they obtained **60a** in a very good yield of 81%. After transmetalation with an excess of BCl_3, they isolated the *para*-isopropyl chloroboracyclohexadiene **61a** in an excellent yield of 98%. Then, the chloroboracyclohexadiene **61a** was treated with two equivalents of $LiNMe_2$. With the first equivalent, the nucleophilic chlorine on the boron is exchanged and the second equivalent deprotonates in *ortho*-position to the boron. Treatment of intermediate **62a** with $Cu^{I}Br$ led then to a coupling in *ortho*-position and offered the corresponding boron dimer. By making use of BCl_3-gas, **62a** was converted into the corresponding boron chloride dimer **63a**. In the last step, pyridazine (**22**) was added dropwise to the boron dimer **63a** and after a thermally allowed suprafacial 1,5-hydrogen shift and the following elimination of TMSCl, the diazadiboratriphenylene **64a** was formed in a yield of 41% (Scheme 15).[71] Later, they also showed that this reaction can be performed with a methyl group in *para*-position to the boron in the cyclohexadiene as well as with other Lewis bases, like phthalazine (**24**), benzo[*c*]cinnoline (**76**) and diphenylpyridazine (Figure 7).[27,71,72]

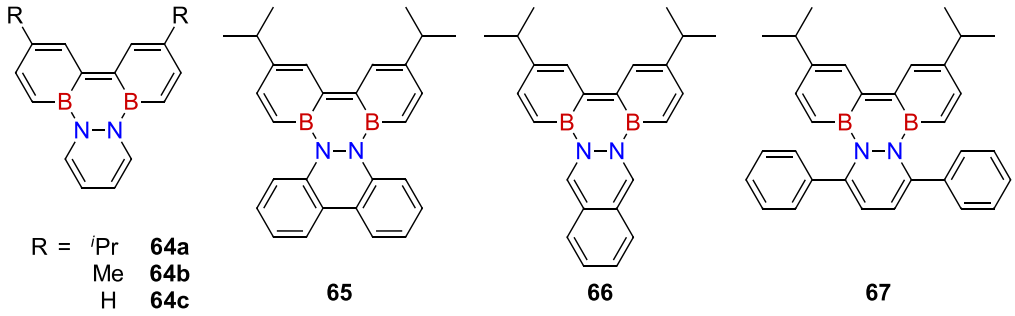

Figure 7: Summarized diazadiboraacences by Piers and co-workers.[27,71,72]

In the case of the unsubstituted diazadiboratriphenylenes **64c** the deprotonation in the *para*-position cannot be avoided. Therefore, they first coupled the cyclohexadiene rings before the transmetalation. This was achieved by treatment of stannacyclohexadiene **59** with LDA for deprotonation (Scheme 16).[27] Afterwards, this intermediate was homo coupled, mediated by iodine, to obtain the dimers **68** and **69** in a ratio of 60:40. In the second step, the dimers **68** and **69** were transmetalated with BCl_3 and afforded the

corresponding boron dimers **63c** and **70** in an overall yield of 60% with **63c** as the major product. In the last step, the mixture of **63c** and **70** was treated with pyridazine (**22**) as Lewis base. A suprafacial 1,5-hydrogen shift led to the elimination of TMSCl and generated the diazadiboratriphenylene **64c** in a yield of 41%.

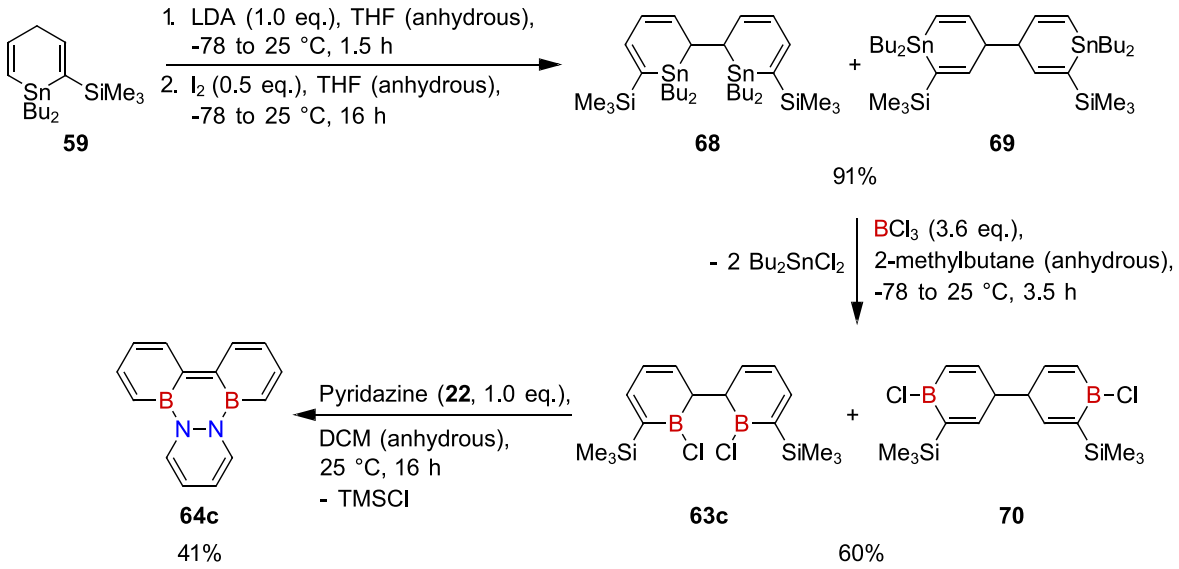

Scheme 16: Synthesis of the unsubstituted diazadiboratriphenylene **64c** starting from stannacyclohexadiene **59** by Piers and co-workers in 2006.[27]

Additionally, they studied the optoelectronic properties of the diazadiboraacences **64a-c** and **65-67**. Compounds **64a-c** all exhibited a strong charge-transfer absorption in the visible region of their UV-Vis spectra, which is also apparent in their highly coloured solutions (Figure 8 – right).[27,71] All UV-Vis spectra of the diazadiboratriphenylenes **64a-c** and **65-67** are red shifted compared to the colorless solution of the all carbon triphenylene (λ_{max} = 258, 275, and 386 nm).[73] In Figure 8, the UV-Vis spectrum of **64c** in cyclohexane is shown in black. The main absorption maximum for **64c** is at 546 nm in a solution of cyclohexane. This absorption is attributed to a charge transfer of an electron from the HOMO, which is primarily located on the $B_2N_2C_2$ ring, to the LUMO, which is located on the two C_5B borabenzene rings. The same transition was observed for the diazadibortriyphenylenes **64a** (545 nm) and **64b** (546 nm). In contrast to **64a-c**, the HOMOs of the compounds **65** and **66** were found to be mainly located on the phthalazine and benzo[*c*]cinnoline parts, while the LUMOs persisted and were largely not effected. Respectively, **65** and **66** are blue-shifted to **64a**, by 43 nm (**65**, λ_{max} = 493 nm) and 70 nm (**66**, λ_{max} = 466 nm). In contrast, **67** is with an absorption maximum of 605 nm red shifted

compared to **64a** by 69 nm, due to exocyclic conjugation effects from the two substituted phenyl groups.[27,74]

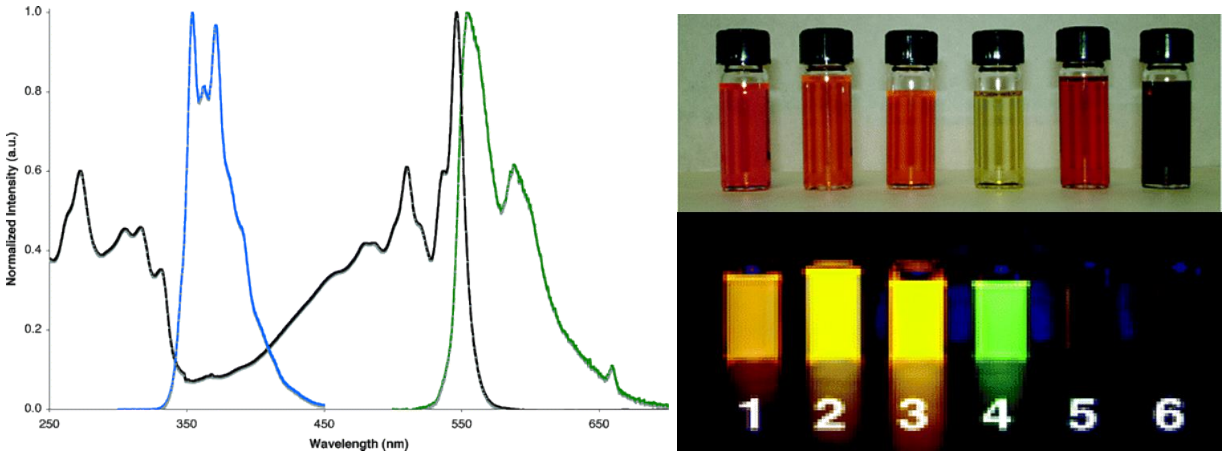

Figure 8: Left: UV-Vis spectrum (black) and the fluorescence spectrum (green) of compound **64c** in *n*-hexane and the fluorescence spectrum of triphenylene in *n*-hexane (blue) all solutions were excited at 260 nm. Right: Picture of diazadiborines triphenylene derivatives solutions in cyclohexane (1 = **64c**; 2 = **64b**; 3 = **64a**, 4 = **66**; 5 = **65**; 6 = **67**) and their visible fluorescence during irradiation at 365 nm.[27]

The excitation of diazadiboratriphenylenes **64a-c** at 260 nm led to red-shifted fluorescence related to all carbon triphenylene (λ_{max} = 355, 363, 372 nm – blue). In the same fashion, all of them exhibited a yellow-orange fluorescence with the main maximum between 551 and 558 nm. The comparison of the fluorescence of **64c** and the all carbon triphenylene is shown in Figure 8. Consequently, small Stokes shift were observed for **64a-c** 12 nm (**64c**), 14 nm (**64b**), and 18 nm (**64a**). This indicates that only a marginal geometric bend occurs in the rigid planar core in the excited state. The excitation of **66** at 260 nm led to a green fluorescence. This blue-shifted emission, relatively to **64a-c**, is in accordance to the blue-shifted UV-Vis spectrum. Nonetheless, **66** has a larger Stokes shift than **64a-c**, which is indicating a larger torsion in the excited state, due to the larger and more flexible core. In the case of **65** and **67** no fluorescence was observed. The aromaticity is reduced, due to the nonplanar twisted geometry, which results from steric repulsion of the 3,3'-hydrogen atoms of the diboraphenyl moiety, either with the 3,3'-H of the benzo[*c*]cinnoline in **65** or 3,3'-H of the hydrogen in *ortho*-position of the phenyl groups on **67**.[27] Nevertheless, all of these compounds could show what a significant influence the B-N-N-B moiety could have on the properties of the carbon backbone.

More recently, the Wegner group published the synthesis of diazadiboranaphthalenes **74a-h**.[75] Starting from 1,2-dibromobenzene (**18**) the bis-pinacolboranebenzene **71** was

synthesized via a Grignard reaction with magnesium and isopropoxy pinacolborane. Afterwards, the borane **71** was reduced with $LiAlH_4$ to obtain the lithium *ortho*-phenylborate **73** in an excellent yield of 91%.[76] The diazadiboranaphthalenes **74a-h** were finally obtained when the lithium *ortho*-phenylborate **73** was reacted with azobenzenes **72a-h** under the elimination of hydrogen, after the *in situ* formation of the corresponding borane with TMSCl. Symmetric electron-rich as well as electron-deficient azobenzenes **74a-e** were used, which led to the corresponding diazadiboranaphthalenes **74a-e** in moderate to good yields (30-63%). Additionally, unsymmetric azobenzenes **74f-h** were used. Here, the yields (15-31%) were lower compared to the symmetrical products **74a-e** (Scheme 17).[75]

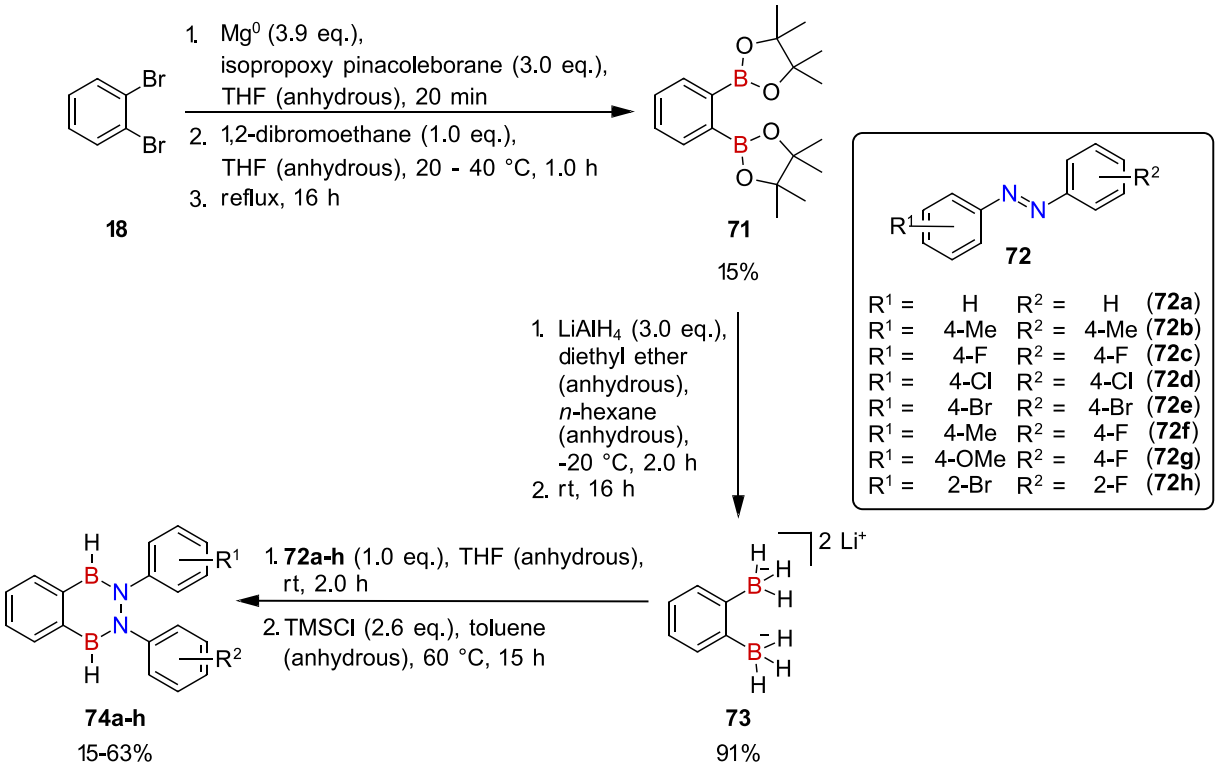

Scheme 17: Synthesis of the diazadiboranaphthalenes **74a-h**.[75]

Additionally, the UV-Vis and fluorescence spectra of the diazadiboranathphtalenes **74a-h** were measured. For comparison, the absorption and fluorescence spectra of **74d** were plotted together with the absorption and fluorescence spectra of the all carbon analogue 2,3-diphenylnaphthalene (**75**) (Figure 9). All spectra were measured as 10^{-5} mol/L solutions in cyclohexane. By comparing the UV-Vis spectra, for **74d** a red-shift of the absorption is observed relative to **75**.[75] But the absorption is similar to the already known

1,2-boraazanaphthalenes **37-42**. Independent of the substitution pattern on the aryl groups, they exhibited roughly the same absorption maximum around 310 nm.[53,55,77] This shows that the local dipole moment of one B-N bond in a smaller aromatic system, like naphthalenes, already has a strong influence on the properties.

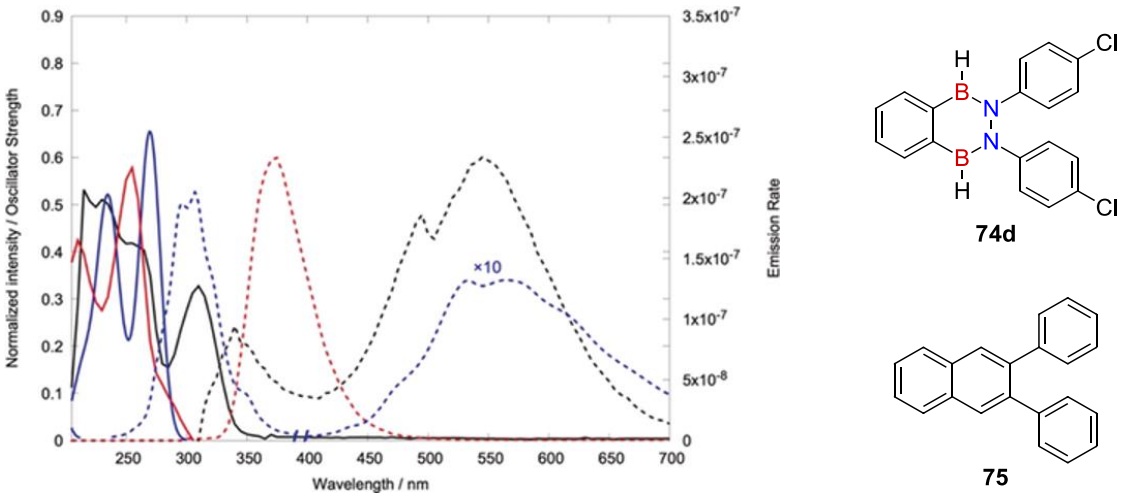

Figure 9: The absorption and emission spectra of the diazadiboranaphthalene **74d** (black lines) and of the all carbon analogue 2,3-diphenylnaphthalene (**75** – red lines). All spectra were measured as solutions in cyclohexane of a concentration of 10^{-5} mol/L. All emission spectra of **74d** were excited at 310 nm and **75** at 354 nm. Additionally, the computed absorption and fluorescence spectra of **74d** are shown (blue lines). The absorption spectra are shown as solid lines and the fluorescence spectra as dotted lines.[75]

For the fluorescence spectrum of **74d** in cyclohexane ($\lambda_{ex.}$ = 310 nm) two emission bands, at 340 and 545 nm, were observed (dotted black line - Figure 9). The large Stokes shift (235 nm) indicates a strong structural torsion in the excited state. Computations showed that $(BN)_2$-naphthlenes **74d** can undergo a twisted intramolecular charge transfer (TICT). In this, the $(C_2B_2N_2)$-unit is twisting and an aryl-ring is flipping into an orthogonal position to the core. This was supported by matrix isolation experiments.[75]

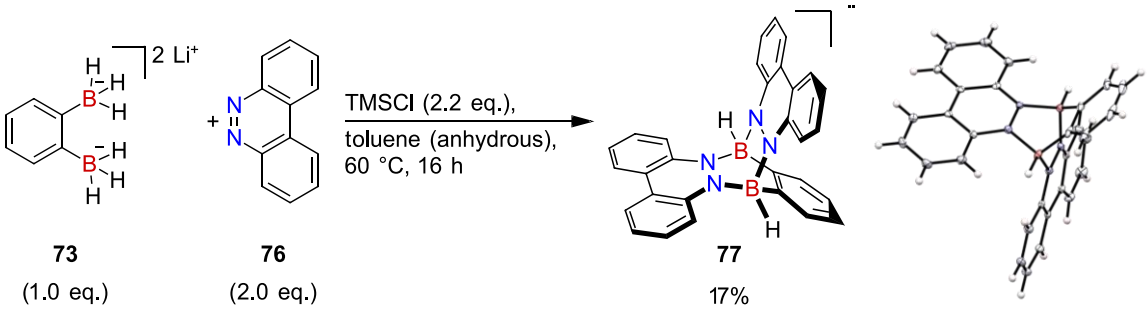

Scheme 18: Synthetic strategy and solid state structure of biradical **77**.[78]

Additionally, the Wegner group showed that treatment of lithium *o*-phenylborate **73** with benzo[*c*]cinnoline (**76**), instead of azobenzenes **72a-h**, leads to a new stable biradical **77**. As discussed earlier, the lithium *o*-phenylborate **73** is converted with TMSCl *in situ* to the corresponding borane. Under the elimination of hydrogen the benzo[*c*]cinnoline (**76**) can react with the borane to the thermally stable biradical **77** (Scheme 18).[78]

In ^{1}H NMR studies of the biradical **77** in a $CDCl_3$ solution, a clear difference could be seen of **77** under the treatment of pyridine (**78**) compare to the initial spectrum of biradical **77**. Within this spectrum signals of the benzo[*c*]cinnoline (**76**) as well as signals related to the pyridine (**78**) stabilized diazaboraacence **79** were also observed. Additionally, the EPR response was weaker than without the addition of pyridine (**78**). Removal of the pyridine (**78**) again provided to the initial ^{1}H NMR and EPR spectra of the biradical **77**. In summary, it could be shown that the dissociation of the second benzo[*c*]cinnoline (**76**) is reversible in solution (Scheme 19).[78]

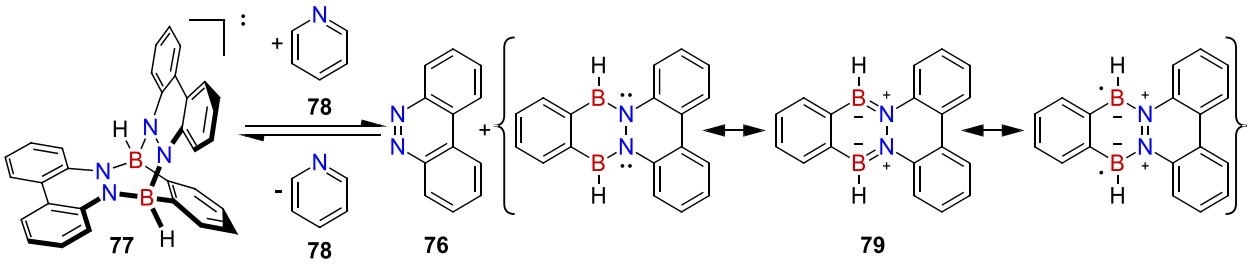

Scheme 19: Reversible formation of biradical **77** under coordination with pyridine (**78**) in solution.[78]

These B-N doped PAHs and the BDLA catalyzed IEDDA reactions, which involves various aspects of boron-nitrogen coordination chemistry, makes it possible to synthesize novel challenging boron-nitrogen materials and access structures which normally couldn't be achieved without transition-metal catalysis.

2. Contribution to Literature

2.1. Synthesis of Medium-Sized Carbocycles via a Bidentate Lewis Acid-Catalyzed Inverse Electron-Demand Diels–Alder Reaction Followed by Photoinduced Ring-Opening

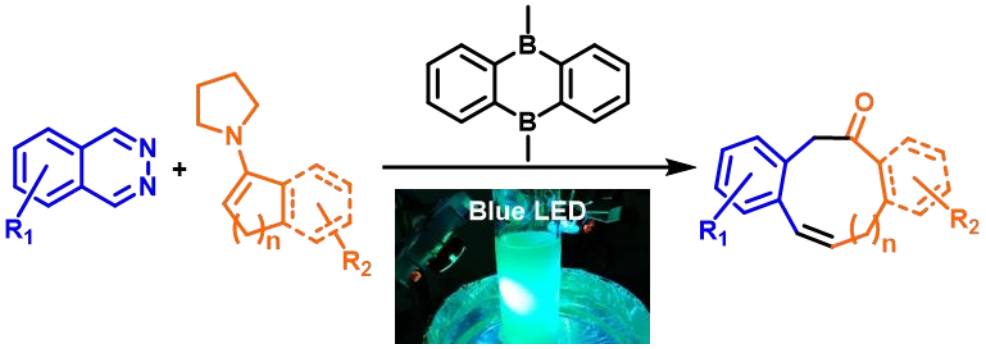

"The combination of a Lewis acid-catalyzed inverse electron-demand Diels–Alder (IEDDA) reaction with a photoinduced ring-opening (PIRO) reaction in a domino process has been established as an efficient synthetic method to access medium-sized carbocycles. From readily available electron-rich and electron-poor phthalazines and enamines, respectively, as starting materials, various 9- and 11-membered carbocycles were prepared. This versatile transition-metal-free tool will be valuable for broadening the structural space in biologically active compounds and functional materials."

Reprinted with permission from
Julia Ruhl, Sebastian Ahles, Marcel A. Strauss, Christopher M. Leonhardt and Hermann A. Wegner
Org. Lett. **2021**, *23*, 2089–2093.
DOI: 10.1021/acs.orglett.1c00249
Publication Date (Web): February 25, 2021

OL Organic Letters

pubs.acs.org/OrgLett Letter

Synthesis of Medium-Sized Carbocycles via a Bidentate Lewis Acid-Catalyzed Inverse Electron-Demand Diels–Alder Reaction Followed by Photoinduced Ring-Opening

Julia Ruhl, Sebastian Ahles, Marcel A. Strauss, Christopher M. Leonhardt, and Hermann A. Wegner*

Cite This: *Org. Lett.* 2021, 23, 2089–2093 Read Online

ABSTRACT: The combination of a Lewis acid-catalyzed inverse electron-demand Diels–Alder (IEDDA) reaction with a photoinduced ring-opening (PIRO) reaction in a domino process has been established as an efficient synthetic method to access medium-sized carbocycles. From readily available electron-rich and electron-poor phthalazines and enamines, respectively, as starting materials, various 9- and 11-membered carbocycles were prepared. This versatile transition-metal-free tool will be valuable for broadening the structural space in biologically active compounds and functional materials.

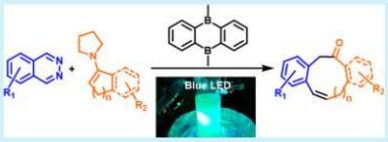

Medium-sized carbon rings (7- to 11-membered) are the structural core motif of various biologically active natural products and medicinally effective synthetic compounds.[1,2] The challenge in creating these medium-sized rings is mostly due to both the ring strain (enthalpy) and the competition between intra- and intermolecular reactions (entropy) during their preparation.[3] Olefin metathesis has been shown to be a very effective method to build these medium-sized rings with either molybdenum (Schrock's)[4,5] or ruthenium (Grubb's)[6,7] catalysts.[8,9] Additionally, it is possible to form medium-sized carbocycles using other metal-catalyzed cyclization, cross-coupling, ring-expansion, and ring-opening reactions as well as free-radical cyclization reactions that rely on metals, such as gallium,[10] platinum,[11,12] cobalt,[13,14] samarium,[15−19] molybdenum,[20] ruthenium,[21,22] indium,[23] manganese,[24,25] iron,[26,27] chromium,[28] copper,[29] palladium,[30,31] silver,[32,33] or gold.[32,34] Further, Nicolaou et al. used a McMurry coupling of a dialdehyde with titanium(III)-chloride in the presence of a zinc–copper couple to build a medium-sized ring system in the total synthesis of taxol.[35] An efficient metal-free method would provide a convenient alternative to access such systems, especially in view of the shortage of resources and sustainability.

In the past, we established bidentate Lewis acids (**BDLA**) as effective catalysts for the inverse electron-demand Diels–Alder (IEDDA) reaction of diazines with various dienophiles.[36] After the initial IEDDA step, a reactive quinodimethane **9** is formed that serves as the ideal base for transformations to various products, such as substituted naphthalenes or complex oligocyclic alkaloid-type structures.[37] The specific outcome of the reaction depends on the conditions chosen and the substitution pattern of the dienophile.[38−41] Recently, we showed that a photoinduced ring-opening (PIRO) reaction of the quinodimethane intermediate **9** by irradiation leads to *ortho*-substituted styrenes. The PIRO reaction of this quinodimethane intermediate **9** proceeds according to the Woodward–Hoffmann rules in a 10π conrotatory pericyclic ring-opening.[42,43] We envisioned that the use of cyclic enamines should deliver medium-sized carbocycles in the same fashion. This would present a metal-free alternative to otherwise difficult-to-prepare targets. Based on our bidentate Lewis acid-catalyzed domino IEDDA/PIRO reaction, we present a modular and transition-metal-free strategy for the synthesis of medium-sized ring systems (Scheme 1).

Scheme 1. Domino Lewis Acid-Catalyzed Inverse Electron-Demand Diels–Alder and Photoinduced Ring-Opening Reaction with Phthalazines 1 and Cyclic Enamines 2

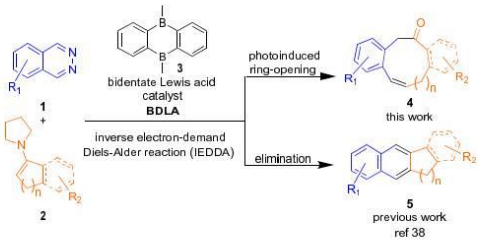

Received: January 21, 2021
Published: February 25, 2021

https://dx.doi.org/10.1021/acs.orglett.1c00249
Org. Lett. 2021, 23, 2089–2093

To realize such a strategy, the **BDLA** catalyst was applied to phthalazine (**1a**) and enamine **2a** under irradiation. First, the reaction mixture was subjected to 448 nm light at different temperatures (see the Supporting Information). Fortunately, the desired 9-membered ring system **4a** was isolated with the eliminated product **5a** as only a minor component. The best yield of 73% was obtained at 80 °C. At higher temperatures, the eliminated IEDDA product **5a** was predominantly formed, decreasing the yield of the photo product **4a**. At temperatures below 80 °C, the IEDDA reaction did not proceed, and the starting material was recovered.

Subsequently, the wavelength was scanned at the optimized temperature of 80 °C. The experiments show that yields above 70% can be achieved with an irradiation between 405 and 500 nm, with an optimum irradiation at 425 nm. As previously shown, the **BDLA** catalyst was partially decomposed at shorter wavelengths (405 nm), significantly reducing the yield.[42] Longer wavelengths between 425 to 500 nm only marginally changed the yield. Hence, a temperature of 80 °C and an irradiation wavelength of 470 nm were chosen as the optimal reaction conditions. At 470 nm, the product was only isolated in a 1% lower yield than at 425 nm, but the purification was much easier due to the formation of fewer side products. As a range of wavelengths from 425 to 500 nm was tolerated, two LEDs were used in some cases to increase the energy density.

To show the scope and high modularity of the IEDDA/PIRO reaction, the reaction was performed with differently substituted starting materials. In the case of 5,8-difluorophthalazine (**1b**), we obtained only the eliminated product under the standard reaction conditions (Figure 1). Due to the lower energy of the lowest unoccupied molecular orbital (LUMO), the IEDDA reaction was expected to proceed much faster. Therefore, the conditions for 5,8-fluorophthalazine (**1b**) were amended to room temperature and an irradiation of 448 and 470 nm. This way, the IEDDA reaction was slower and the PIRO reaction could compete with the elimination. With the same refinement, the reaction of 6-fluorophthalazine (**1c**) was performed at 30 °C with an irradiation of 425 and 470 nm. For the same reason, the IEDDA/PIRO reactions with 6-(trifluoromethyl)phthalazine (**1d**) and 6-chlorophthalazine (**1e**) were done at the same irradiation wavelengths and lower temperatures compared to those of the unsubstituted phthalazine (**1a**). Due to the lower reaction temperatures for the electron-poor phthalazines **1b−d**, the corresponding eliminated products were not obtained. In these cases, the remaining phthalazine starting materials **1b−d** were recovered. In case of 6-chlorophthalazine **1e**, the reaction temperature had to be raised to 50 °C for an optimal yield. This produced the eliminated product **5e** as a side product. For all electron-deficient phthalazines **1b−e**, the corresponding 9-membered carbocycles **4b−e** were obtained in good to very good yields. The IEDDA/PIRO reaction with the electron-rich 6-methoxyphthalazine (**1f**) had to be performed at 130 °C and an irradiation of 425 and 448 nm. However, the corresponding photo product **4f** was only obtained in a yield of 5%. Because of the higher LUMO energy of the 6-methoxyphthalazine (**1f**), more energy (higher temperature) was needed for the initial IEDDA reaction, favoring the elimination reaction. Additionally, we used 6-methylphthalazine, 6,7-dimethylphthalazine, and 6,7-dimethoxyphthalazine in the IEDDA/PIRO reaction. However, only the starting materials were reisolated in all three cases. Due to the energetically higher LUMO energy of the phthalazine derivatives, the IEDDA reaction did not proceed for these starting materials.

Next, different cyclic enamines **2b−f** were screened (Figure 2). All enamines **2a−f** were synthesized following a known procedure reported by Thompson et al.[44] The PIRO reaction proceeded smoothly with unsubstituted 1-(1-cyclopenten-1-yl)pyrrolidine (**2b**). Due to the lower steric hindrance of enamine **2b**, it was possible to obtain the (7*Z*)-bicyclo[7.4.0]-trideca-1(13),7,9,11-tetraen-3-one (**4g**) product in an excellent yield of 93%. Additionally, electron-rich and electron-deficient

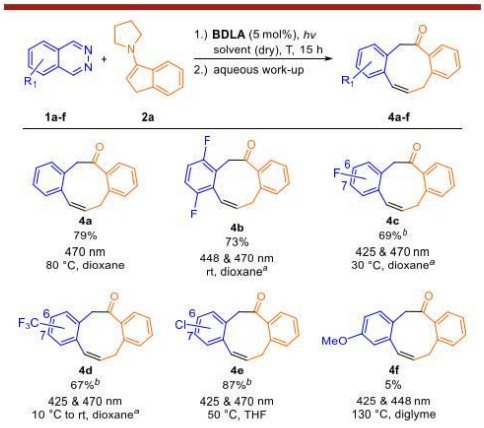

Figure 1. Screening of the phthalazines **1a−f** in the IEDDA/PIRO reaction with enamine **2a**. Reaction conditions are as follows: phthalazines (**1a−f**) (1.0 mmol, 1.0 equiv), **BDLA** (50 μmol, 5.0 mol %), enamine **2a** (2.9 mmol, 2.9 equiv), and dry solvents (10 mL, 100 mM). [a]The corresponding eliminated product was not obtained under these reaction conditions. [b]Isolated yield as mixture of C6 and C7 constitutional isomers.

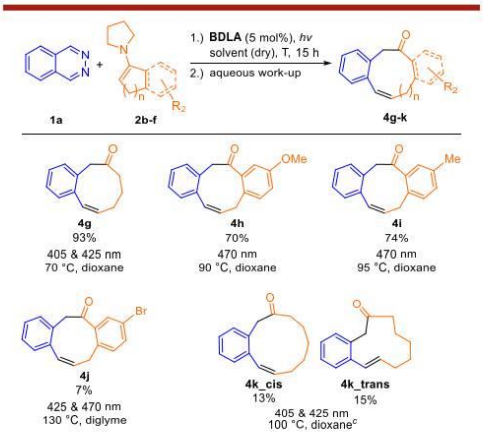

Figure 2. Screening of the cyclic enamines **2b−f** in the IEDDA/PIRO reaction with phthalazine **1a**. Reaction conditions are as follows: phthalazine (**1a**) (1.0 mmol, 1.0 equiv), **BDLA** (50 μmol, 5.0 mol%), enamines **2b−f** (2.9 mmol, 2.9 equiv), and dry solvents (10 mL, 100 mM). [c]**BDLA** (0.10 mmol, 10 mol %) was used as a catalyst.

https://dx.doi.org/10.1021/acs.orglett.1c00249
Org. Lett. 2021, 23, 2089−2093

enamines could be used in the IEDDA/PIRO reaction; 1-(6-methoxy-3*H*-inden-1-yl)pyrrolidine (**2c**) and 1-(6-methly-3*H*-inden-1-yl)pyrrolidine (**2d**), respectively, were converted to the corresponding photo products **4h** and **4i** in good yields. For the 5-bromo-substituted enamine **2e**, the reaction temperature was increased to 130 °C and the irradiation was done at 425 and 470 nm. Again, the elimination reaction was preferred in this case due to the harsher conditions, and the corresponding photo product **4j** was only isolated in a yield of 7%.

Enamines with an increased ring size would give access to even larger carbocycles. For example, the IEDDA/PIRO reaction of phthalazine (**1a**) and 1-(1-cyclohepten-1-yl)-pyrrolidine (**2f**) provided the 11-membered carbocycle **4k**, although in lower yields and as both double-bond isomers. To obtain a better understanding of why the synthesis of **4k** yielded both isomers and that of **4g** yielded a single isomer, a computational analysis was conducted. Therefore, conformer ensembles of compounds **4k_cis**, **4k_trans**, **4g_cis**, and the theoretical **4g_trans** were computed with the Conformer–Rotamer Ensemble Sampling Tool (CREST)[45,46] developed by Grimme and co-workers. The structures of the conformer with the lowest energy were further optimized on the PBE0[47] level of theory with a def2-TZVP[48] basis set and the D3-BJ[49,50] dispersion correction. High-level single-point corrections were computed at the DLPNO–CCSD(T)[51] level, also using the def2-TZVP basis set. This computational analysis showed that the difference in $\Delta G°$ between **4k_cis** and **4k_trans** was merely 0.37 kcal/mol. For **4g** and its theoretical *trans*-isomer, this difference increased to 4.20 kcal/mol due to the higher ring strain, clearly favoring the formation of a bowl-shaped structure of the *cis*-isomer over the less favorable *trans*-isomer (see the Supporting Information for more details). The lower yield can be rationalized by the decomposition of the **BDLA** over time, as the IEDDA reaction proceeded much slower.[42] Furthermore, both 1-(1-cyclohexen-1-yl)pyrrolidine and 1-(1-cycloocten-1-yl)pyrrolidine were tested in the IEDDA/PIRO reaction. However, these substrates did not react in the IEDDA, probably due to the increased steric demand of these enamines. In previous publications, we also showed that these enamines need higher temperatures to undergo the IEDDA reaction and form the corresponding eliminated products.[38,52] Therefore, we also tested the IEDDA/PIRO reaction with the two isomeric six-membered enamines 1-(3,4-dihydronaphth-1-yl)pyrrolidine and 1-(3,4-dihydronaphth-2-yl)pyrrolidine. These reaction partners should have more planar ring systems than 1-(1-cyclohexen-1-yl)pyrrolidine, reducing the steric hindrance. However, the IEDDA reaction also did not proceed in these cases.

The method can easily be carried out on a gram scale. The reaction of phthalazine (**1a**) and enamine **2b** was set up in a Schlenk tube, and the reaction mixture was irradiated with two LEDs (470 and 500 nm). However, the larger diameter of the reaction vessel reduced the penetration depth of the light, favoring side reactions. Hence, the photo product **4a** was obtained in a lower yield of 57% compared to that of the small scale.

Additionally, the IEDDA/PIRO reaction of phthalazine (**1a**) and enamine **2a** was performed with the air-stable variant of the bidentate Lewis acid catalyst recently developed by us (see Supporting Information for details).[53] In this case, the reaction temperature was slightly increased to 90 °C to speed up the exchange of the coordinated pyridazine on the bidentate Lewis acid with the phthalazine reactant (**1a**). Nevertheless, the desired photo product **4a** was isolated in a 61% yield.

Based on previous studies of the IEDDA reaction, the following mechanistic proposal is put forward for the IEDDA/PIRO reaction. In the first step of the catalytic cycle, the bidentate Lewis acid **3** coordinates to the phthalazine (**1a**) to form complex **6**.[37] The activated phthalazine can now react with an electron-rich dienophile, in this case enamine **7**, to form the intermediate **8** via an IEDDA reaction. The elimination of nitrogen regenerates the BDLA and leads to the quinodimethane intermediate **9**.[37,40] For the ring-opening, a visible-light-promoted opening of the quinodimethane intermediate **9** to enamine **10** is hypothesized.[42] With 10π electrons involved, this photo electrocyclization reaction has to proceed conrotatory according to the Woodward–Hoffmann rules.[43,54] The cyclic enamine **10** is transformed to the corresponding cyclic ketone **11** during aqueous workup (Scheme 2).

Scheme 2. Catalytic Cycle of the Domino Bidentate Lewis Acid-Catalyzed IEDDA Reaction of Phthalazine (1a) and an Electron-Rich Dienophile 7[a]

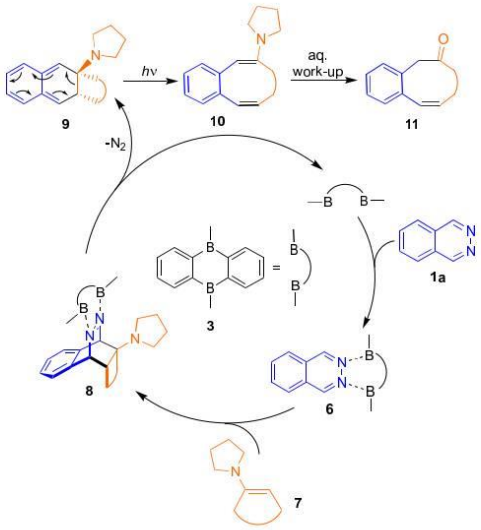

[a]The catalytic cycle was followed by the photoinduced ring-opening (PIRO) reaction.

In summary, we established the IEDDA/PIRO reaction of phthalazines and cyclic enamines as a powerful tool for the synthesis of medium-sized carbocycles. The scope of this reaction was shown by screening differently substituted phthalazines **1a–f** and cyclic enamines **2a–f**. We demonstrated that the electron-rich enamines **2c** and **2d** and especially the electron-deficient phthalazines **1b–e** provided the corresponding medium-sized carbocycles in good to very good yields. However, the electron-rich phthalazine **1f** and electron-deficient enamine **2e** only reacted sluggishly in the domino IEDDA/PIRO reaction. By using enamines with different ring-sizes, it was shown that sterics also influence the IEDDA/PIRO reaction. Over all, the IEDDA/PIRO reaction offers a

https://dx.doi.org/10.1021/acs.orglett.1c00249
Org. Lett. 2021, 23, 2089–2093

new transition-metal-free and stereoselective synthesis strategy for 9- and 11-membered carbocycles, which will contribute to the efficient expansion of the molecular space for biological and materials applications.[55−57]

■ ASSOCIATED CONTENT

Supporting Information

The Supporting Information is available free of charge at https://pubs.acs.org/doi/10.1021/acs.orglett.1c00249.

Experimental details, analytical data, NMR spectra, and computational details (PDF)

■ AUTHOR INFORMATION

Corresponding Author

Hermann A. Wegner − *Institute of Organic Chemistry, Justus Liebig University Giessen, 35392 Giessen, Germany; Center for Materials Research (LaMa), Justus Liebig University Giessen, 35392 Giessen, Germany;* orcid.org/0000-0001-7260-6018; Email: hermann.a.wegner@org.chemie.uni-giessen.de

Authors

Julia Ruhl − *Institute of Organic Chemistry, Justus Liebig University Giessen, 35392 Giessen, Germany; Center for Materials Research (LaMa), Justus Liebig University Giessen, 35392 Giessen, Germany;* orcid.org/0000-0002-3062-9227

Sebastian Ahles − *Institute of Organic Chemistry, Justus Liebig University Giessen, 35392 Giessen, Germany; Center for Materials Research (LaMa), Justus Liebig University Giessen, 35392 Giessen, Germany;* orcid.org/0000-0002-3954-5513

Marcel A. Strauss − *Institute of Organic Chemistry, Justus Liebig University Giessen, 35392 Giessen, Germany; Center for Materials Research (LaMa), Justus Liebig University Giessen, 35392 Giessen, Germany;* orcid.org/0000-0001-8152-9421

Christopher M. Leonhardt − *Institute of Organic Chemistry, Justus Liebig University Giessen, 35392 Giessen, Germany; Center for Materials Research (LaMa), Justus Liebig University Giessen, 35392 Giessen, Germany*

Complete contact information is available at: https://pubs.acs.org/10.1021/acs.orglett.1c00249

Notes

The authors declare no competing financial interest.

■ ACKNOWLEDGMENTS

We thank Heike Hausmann (Justus Liebig University, Giessen) for NMR support and Edgar Reitz (Justus Liebig University, Giessen) for the design and construction of the LED devices.

■ REFERENCES

(1) Hussain, A.; Yousuf, S. K.; Mukherjee, D. Importance and synthesis of benzannulated medium-sized and macrocyclic rings (BMRs). *RSC Adv.* **2014**, *4*, 43241−43257.

(2) Nicolaou, K. C.; Vourloumis, D.; Winssinger, N.; Baran, P. S. The Art and Science of Total Synthesis at the Dawn of the Twenty-First Century. *Angew. Chem., Int. Ed.* **2000**, *39*, 44−122.

(3) Galli, C.; Mandolini, L. The Role of Ring Strain on the Ease of Ring Closure of Bifunctional Chain Molecules. *Eur. J. Org. Chem.* **2000**, *2000*, 3117−3125.

(4) Schrock, R. R. Multiple metal-carbon bonds for catalytic metathesis reactions (Nobel Lecture). *Angew. Chem., Int. Ed.* **2006**, *45*, 3748−3759.

(5) McConville, D. H.; Wolf, J. R.; Schrock, R. R. Synthesis of chiral molybdenum ROMP initiators and all-cis highly tactic poly(2,3-(R)2norbornadiene) (R = CF3 or CO2Me). *J. Am. Chem. Soc.* **1993**, *115*, 4413−4414.

(6) Grubbs, R. H. Olefin-metathesis catalysts for the preparation of molecules and materials (Nobel Lecture). *Angew. Chem., Int. Ed.* **2006**, *45*, 3760−3765.

(7) Ogba, O. M.; Warner, N. C.; O'Leary, D. J.; Grubbs, R. H. Recent advances in ruthenium-based olefin metathesis. *Chem. Soc. Rev.* **2018**, *47*, 4510−4544.

(8) Yet, L. Metal-mediated synthesis of medium-sized rings. *Chem. Rev.* **2000**, *100*, 2963−3008.

(9) Maier, M. E. Synthesis of Medium-Sized Rings by the Ring-Closing Metathesis Reaction. *Angew. Chem., Int. Ed.* **2000**, *39*, 2073−2077.

(10) Kim, S. M.; Lee, S. I.; Chung, Y. K. GaCl3-catalyzed formation of eight-membered rings from enynes bearing a cyclic olefin. *Org. Lett.* **2006**, *8*, 5425−5427.

(11) Fürstner, A.; Davies, P. W. Catalytic carbophilic activation: catalysis by platinum and gold pi acids. *Angew. Chem., Int. Ed.* **2007**, *46*, 3410−3449.

(12) Añorbe, L.; Domínguez, G.; Pérez-Castells, J. Reorganization of enynes catalyzed by platinum salts. *Chem. - Eur. J.* **2004**, *10*, 4938−4943.

(13) Bradley, A.; Motherwell, W. B.; Ujjainwalla, F. A concise approach towards the synthesis of steganone analogues. *Chem. Commun.* **1999**, 917−918.

(14) Jamison, T. F.; Shambayati, S.; Crowe, W. E.; Schreiber, S. L. Tandem Use of Cobalt-Mediated Reactions to Synthesize (+)-Epoxydictymene, a Diterpene Containing a Trans -Fused 5−5 Ring System. *J. Am. Chem. Soc.* **1997**, *119*, 4353−4363.

(15) Molander, G. A.; Etter, J. B.; Harring, L. S.; Thorel, P. J. Investigations on 1,2-, 1,3-, and 1,4-asymmetric induction in intramolecular Reformatskii reactions promoted by samarium(II) iodide. *J. Am. Chem. Soc.* **1991**, *113*, 8036−8045.

(16) Molander, G. A.; Harris, C. R. Sequenced Reactions with Samarium(II) Iodide. Tandem Intramolecular Nucleophilic Acyl Substitution/Intramolecular Barbier Cyclizations. *J. Am. Chem. Soc.* **1995**, *117*, 3705−3716.

(17) Matsuda, F.; Kito, M.; Sakai, T.; Okada, N.; Miyashita, M.; Shirahama, H. Efficient construction of 8-membered ring framework of vinigrol through SmI2-induced coupling cyclization. *Tetrahedron* **1999**, *55*, 14369−14380.

(18) Berndt, M.; Gross, S.; Hölemann, A.; Reissig, H.-U. New Samarium Diiodide-Induced Ketyl Couplings - From Analogous Reactions to Serendipitously Discovered Processes. *Synlett* **2004**, 422−438.

(19) Molander, G. A.; McKie, J. A. Samarium(II) iodide-induced reductive cyclization of unactivated olefinic ketones. Sequential radical cyclization/intermolecular nucleophilic addition and substitution reactions. *J. Org. Chem.* **1992**, *57*, 3132−3139.

(20) Yin, J.; Liebeskind, L. S. Enantiocontrolled [5 + 2] Cycloaddition to η 3 -Pyranylmolybdenum π-Complexes. Synthesis of Substituted Oxabicyclo[3.2.1]octenes of High Enantiopurity. *J. Am. Chem. Soc.* **1999**, *121*, 5811−5812.

(21) Wender, P. A.; Fuji, M.; Husfeld, C. O.; Love, J. A. Rhodium-Catalyzed [5 + 2] Cycloadditions of Allenes and Vinylcyclopropanes. *Org. Lett.* **1999**, *1*, 137−140.

(22) Wender, P. A.; Husfeld, C. O.; Langkopf, E.; Love, J. A. First Studies of the Transition Metal-Catalyzed [5 + 2] Cycloadditions of Alkenes and Vinylcyclopropanes. *J. Am. Chem. Soc.* **1998**, *120*, 1940−1941.

(23) Cintas, P. Synthetic Organoindium Chemistry. *Synlett* **1995**, *1995*, 1087−1096.
(24) Snider, B. B. Manganese(III)-Based Oxidative Free-Radical Cyclizations. *Chem. Rev.* **1996**, *96*, 339−364.
(25) Snider, B. B.; Merritt, J. E. Formation of seven- and eight-membered rings by Mn(III)-based oxidative free-radical cyclization. *Tetrahedron* **1991**, *47*, 8663−8678.
(26) Booker-Milburn, K. I.; Thompson, D. F. Iron(III) mediated transformations of cyclopropyltrimethylsilyl ethers. Part 1. Free radical tandem ring expansion−cyclisation reactions for the rapid construction of [n.3.0] bicyclic ring systems. *J. Chem. Soc., Perkin Trans. 1* **1995**, *45*, 2315−2321.
(27) Christoffers, J. Iron(III) catalysis of an intramolecular Michael reaction. *Tetrahedron Lett.* **1998**, *39*, 7083−7084.
(28) Fürstner, A. Carbonminus signCarbon Bond Formations Involving Organochromium(III) Reagents. *Chem. Rev.* **1999**, *99*, 991−1046.
(29) de Campo, F.; Lastécouères, D.; Verlhac, J.-B. New and improved catalysts for transition metal catalysed radical reactions. *Chem. Commun.* **1998**, *1998* (19), 2117−2118.
(30) Ohno, H.; Hamaguchi, H.; Ohata, M.; Kosaka, S.; Tanaka, T. Palladium(0)-catalyzed synthesis of medium-sized heterocycles by using bromoallenes as an allyl dication equivalent. *J. Am. Chem. Soc.* **2004**, *126*, 8744−8754.
(31) Denmark, S. E.; Yang, S.-M. Sequential ring-closing metathesis/Pd-catalyzed, Si-assisted cross-coupling reactions. *Tetrahedron* **2004**, *60*, 9695−9708.
(32) Watson, I. D. G.; Ritter, S.; Toste, F. D. Asymmetric synthesis of medium-sized rings by intramolecular Au(I)-catalyzed cyclopropanation. *J. Am. Chem. Soc.* **2009**, *131*, 2056−2057.
(33) Muñoz, M. P. Silver and platinum-catalysed addition of O-H and N-H bonds to allenes. *Chem. Soc. Rev.* **2014**, *43*, 3164−3183.
(34) Jiménez, T.; Carreras, J.; Ceccon, J.; Echavarren, A. M. Gold(I)-Catalyzed Inter- and Intramolecular Additions of Carbonyl Compounds to Allenenes. *Org. Lett.* **2016**, *18*, 1410−1413.
(35) Nicolaou, K. C.; Yang, Z.; Liu, J. J.; Ueno, H.; Nantermet, P. G.; Guy, R. K.; Claiborne, C. F.; Renaud, J.; Couladouros, E. A.; Paulvannan, K.; Sorensen, E. J. Total synthesis of taxol. *Nature* **1994**, *367*, 630−634.
(36) Schweighauser, L.; Wegner, H. A. Bis-Boron Compounds in Catalysis: Bidentate and Bifunctional Activation. *Chem. - Eur. J.* **2016**, *22*, 14094−14103.
(37) Schweighauser, L.; Bodoky, I.; Kessler, S. N.; Häussinger, D.; Donsbach, C.; Wegner, H. A. Bidentate Lewis Acid Catalyzed Domino Diels-Alder Reaction of Phthalazine for the Synthesis of Bridged Oligocyclic Tetrahydronaphthalenes. *Org. Lett.* **2016**, *18*, 1330−1333.
(38) Kessler, S. N.; Neuburger, M.; Wegner, H. A. Bidentate Lewis Acids for the Activation of 1,2-Diazines - A New Mode of Catalysis. *Eur. J. Org. Chem.* **2011**, *2011*, 3238−3245.
(39) Kessler, S. N.; Neuburger, M.; Wegner, H. A. Domino inverse electron-demand Diels-Alder/cyclopropanation reaction of diazines catalyzed by a bidentate Lewis acid. *J. Am. Chem. Soc.* **2012**, *134*, 17885−17888.
(40) Kessler, S. N.; Wegner, H. A. One-pot synthesis of phthalazines and pyridazino-aromatics: a novel strategy for substituted naphthalenes. *Org. Lett.* **2012**, *14*, 3268−3271.
(41) Ahles, S.; Götz, S.; Schweighauser, L.; Brodsky, M.; Kessler, S. N.; Heindl, A. H.; Wegner, H. A. An Amine Group Transfer Reaction Driven by Aromaticity. *Org. Lett.* **2018**, *20*, 7034−7038.
(42) Ahles, S.; Ruhl, J.; Strauss, M. A.; Wegner, H. A. Combining Bidentate Lewis Acid Catalysis and Photochemistry: Formal Insertion of o-Xylene into an Enamine Double Bond. *Org. Lett.* **2019**, *21*, 3927−3930.
(43) Woodward, R. B.; Hoffmann, R. Stereochemistry of Electrocyclic Reactions. *J. Am. Chem. Soc.* **1965**, *87*, 395−397.
(44) Thompson, H. W.; Huegi, B. S. Stabilised enamine anions. Generation and alkylation of anions stabilised as cyclopentadienide enamine systems. *J. Chem. Soc., Perkin Trans. 1* **1976**, 1603−1607.
(45) Pracht, P.; Bohle, F.; Grimme, S. Automated exploration of the low-energy chemical space with fast quantum chemical methods. *Phys. Chem. Chem. Phys.* **2020**, *22*, 7169−7192.
(46) Grimme, S. Exploration of Chemical Compound, Conformer, and Reaction Space with Meta-Dynamics Simulations Based on Tight-Binding Quantum Chemical Calculations. *J. Chem. Theory Comput.* **2019**, *15*, 2847−2862.
(47) Adamo, C.; Barone, V. Toward reliable density functional methods without adjustable parameters. *J. Chem. Phys.* **1999**, *110*, 6158−6170.
(48) Weigend, F.; Ahlrichs, R. Balanced basis sets of split valence, triple zeta valence and quadruple zeta valence quality for H to Rn: Design and assessment of accuracy. *Phys. Chem. Chem. Phys.* **2005**, *7*, 3297−3305.
(49) Grimme, S.; Ehrlich, S.; Goerigk, L. Effect of the damping function in dispersion corrected density functional theory. *J. Comput. Chem.* **2011**, *32*, 1456−1465.
(50) Grimme, S.; Antony, J.; Ehrlich, S.; Krieg, H. A consistent and accurate ab initio parametrization of density functional dispersion correction (DFT-D) for the 94 elements H-Pu. *J. Chem. Phys.* **2010**, *132*, 154104.
(51) Riplinger, C.; Sandhoefer, B.; Hansen, A.; Neese, F. Natural triple excitations in local coupled cluster calculations with pair natural orbitals. *J. Chem. Phys.* **2013**, *139*, 134101.
(52) Balcar, J.; Chrisam, G.; Huber, F. X.; Sauer, J. Reaktivität von stickstoff-heterocyclen genenüber cyclooctin als dienophil. *Tetrahedron Lett.* **1983**, *24*, 1481−1484.
(53) Hong, L.; Ahles, S.; Heindl, A. H.; Tiétcha, G.; Petrov, A.; Lu, Z.; Logemann, C.; Wegner, H. A. An air-stable bisboron complex: a practical bidentate Lewis acid catalyst. *Beilstein J. Org. Chem.* **2018**, *14*, 618−625.
(54) Woodward, R. B.; Hoffmann, R. The Conservation of Orbital Symmetry. *Angew. Chem., Int. Ed. Engl.* **1969**, *8*, 781−853.
(55) Rabinovitz, M.; Willner, I.; Gamliel, A.; Gazit, A. Benzannelated [9] and [13] annulenes. *Tetrahedron* **1979**, *35*, 667−673.
(56) Rabinovitz, M.; Willner, I. Aromatic linearly annelated dibenzocyclononatetraenyl anion. *Tetrahedron Lett.* **1974**, *15*, 4447−4450.
(57) Kajioka, T.; Ikai, M.; Fujikawa, H.; Taga, Y. Disubstituted 1,6-methano[10]annulene derivatives for use in organic light-emitting diodes. *Tetrahedron* **2004**, *60*, 6183−6187.

https://dx.doi.org/10.1021/acs.orglett.1c00249
Org. Lett. 2021, 23, 2089−2093

2.2. Diazadiboraacenes: Synthesis, Spectroscopy and Computations

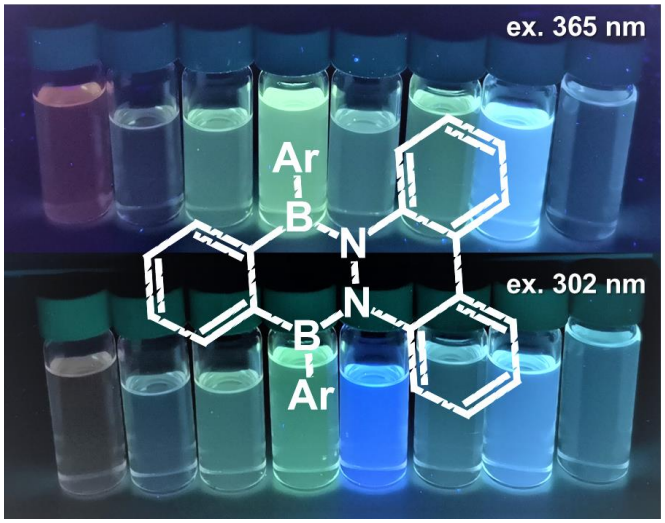

“The incorporation of heteroatoms into hydrocarbon compounds greatly expands the chemical space of molecular materials. In this context, B-N doping takes a center stage due to its isosterism with a C=C-bond. Herein, we present a new and modular synthetic concept to access novel diazadiborabenzo[*b*]triphenylenes **7a-h** using the B-N doped biradical **16** as intermediate. Characterization of the photophysical properties revealed the emission spectra of the diazadibora benzo[*b*]triohenylenes **7a-h** can conveniently be tuned by small changes of the substitution on the boron-atom. All of the diazadibora compounds show a short life-time phosphorescence. Additionally, we were able to rationalize the excited-state relaxation of the diazadiboraacene **7a** via intersystem crossing by quantum chemical calculations. The new synthetic strategy provides an elegant route to various novel B-N doped acenes with great potential for applications in molecular materials.”

Reprinted with permission from
Julia Ruhl, Nils Oberhof, Andreas Dreuw and Hermann A. Wegner
Angew. Chem. Int. Ed. **2023**, e202300785.
DOI: 10.1002/anie.202300785
Publication Date (Web): February 13, 2023

Angewandte Chemie International Edition 10.1002/anie.202300785

WILEY-VCH

COMMUNICATION

Diazadiboraacenes: Synthesis, Spectroscopy and Computations

Julia Ruhl,[a,b] Nils Oberhof,[c] Andreas Dreuw,[c] and Hermann A. Wegner*[a,b]

[a] J. Ruhl, Prof. Dr. H. A. Wegner
Institute of Organic Chemistry
Justus Liebig University Giessen
Heinrich-Buff-Ring 17, 35392 Giessen, Germany
E-mail: Hermann.A.Wegner@org.chemie.uni-giessen.de

[b] J. Ruhl, Prof. Dr. H. A. Wegner
Center for Materials Research (LaMa)
Justus Liebig University Giessen
Heinrich-Buff-Ring 16, 35392 Giessen, Germany

[c] N. Oberhof, Prof. Dr. A. Dreuw
Interdisciplinary Center for Scientic Computing
Heidelberg University
Im Neuenheimer Feld 205, 69120 Heidelberg, Germany

Supporting information for this article is given via a link at the end of the document.

Abstract: The incorporation of heteroatoms into hydrocarbon compounds greatly expands the chemical space of molecular materials. In this context, B-N doping takes a center stage due to its isosterism with a C=C-bond. Herein, we present a new and modular synthetic concept to access novel diazadiborabenzo[*b*]triphenylenes **7a-h** using the B-N doped biradical **16** as intermediate. Characterization of the photophysical properties revealed the emission spectra of the diazadibora benzo[*b*]triohenylenes **7a-h** can conveniently be tuned by small changes of the substitution on the boron-atom. All of the diazadibora compounds show a short life-time phosphorescence. Additionally, we were able to rationalize the excited-state relaxation of the diazadiboraacene **7a** via intersystem crossing by quantum chemical calculations. The new synthetic strategy provides an elegant route to various novel B-N doped acenes with great potential for applications in molecular materials.

Polycyclic aromatic hydrocarbons (PAHs) have received noteworthy attention in materials research due to their application potential, e.g. in organic light emitting diodes (OLEDs),[1] organic field-effect transistors (OFETs),[2] or solar cells.[3] This is *inter alia* related to their versatile structure dependent properties and their modular synthetic access.[4] Further, the implementation of boron in PAHs was shown to lead to new exceptional optoelectronic materials.[5,6] By introducing one boron and one nitrogen next to each other in PAHs, the resulting compounds are isosteric and isoelectronic to the all-carbon analogue (B−N/C=C isoterism). This does however introduce, a dipole moment in the PAH, which can significantly influence the solid-state structure as well as electronic and optoelectronic properties but the existing molecular structural features are maintained. These changes are due to the modification of the gap between the highest occupied and lowest unoccupied molecular orbital (HOMO and LUMO), as well as the intermolecular interactions in the solid state.[5,7]

Pioneers of this concept were Dewar *et al.*,[8] who already presented the synthesis of various diazadibora-analogues of pyrene and anthracene **1** in the 1950s and 1960s (Figure 1).[9] In addition, they also presented the synthesis of azabora-naphthalene and phenanthrene, in which the isoelectronic B−N moieties replaced C=C positions at the perimeter of the compounds. Notwithstanding of the useful properties of B,N doped acenes and their role in PAH chemistry, it took over 50 years until parental BN isosteres of higher acenes, besides the bicyclic naphthalene, have been reported.[10] For example, in 2014 Chrostowska and co-workers showed a new synthesis to implement B−N moieties in anthracene systems and the properties of these B,N-anthracenes **2**.[11] In 2021, Tian *et al.* reported a novel synthesis of 9,9a-B,N anthracene derivatives **3** along with its photophysical properties.[12]

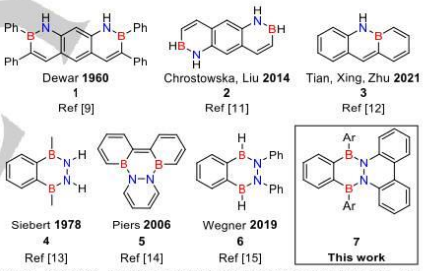

Figure 1. Selection of six-membered BN isosteres of anthracene and BN isosteres of PAHs with a $C_2B_2N_2$ core.

In most cases of B,N-PAHs the B−N units are spatially separated by multiple carbon bonds. In this way, separated polar bonds are implemented in the molecules leading mostly to a weak additional dipole moment. However, when the two B−N bonds are, connected via the N-atoms, in the molecular structure, the combined polar bonds should lead to a stronger overall dipole moment of the molecule. The first synthesis of such diazadiboracenes were reported by Siebert and co-worker with the example of the 2,3,1,4-diazadibora naphthalenes **4** in 1978.[13] Piers and co-workers reported the same pattern incorporated inside a triphenylene unit.[14,15] They investigated the synthesis and the photophysical properties of diazadiboratriphenylene **5**. By introducing different diazines to their boron precursor they were able to alter the photophysical and electronic properties of these compounds. In addition, they observed short B••N intermolecular coordination in crystal structure. This strengthened the (π)-stacking of the triphenylene **5**, which could lead to better electron transport in electronic materials.

Angewandte Chemie International Edition 10.1002/anie.202300785

WILEY-VCH

COMMUNICATION

Recently, our group reported a synthetic route to diazadiboranaphthalenes **6** and investigated their photophysical properties.[16] In these studies, we were able to show that the diazadiboranaphthalenes **6** exhibits two solvent-dependent emissions, and the one at longer wavelength was attributed to a twisted intramolecular charge transfer (TICT). This TICT behavior was supported by computations and matrix-isolation experiments. Furthermore, in 2017 we showed the synthesis and properties of an B,N-based stable biradical **16**.[17] Interestingly, we could demonstrate by ^{1}H NMR spectroscopy that in the presence of a competing ligand, such as pyridine, the second coordination of the benzo[*c*]cinnoline (**15**) is reversible in solution and in equilibrium with pyridine. However, the diazadiborabenzo-[*b*]triphenylene backbone was only observed spectroscopically and could not be isolated.

Herein, we present the preparation and investigation of novel diazadiborabenzo[*b*]triphenylenes **7a-h**. We started first with the synthesis goal of an air-stable diazadibora benzo[*b*]triphenylene. In general, there are two possible strategies to stabilize a trivalent boron in PAHs. The first one is the "principle of structural constraint".[18] In this approach, the boron is stabilized by embedding it into the inner part of PAHs. As a result, tetra-coordinated adducts of the boron become unfavorable and C−B bond cleavage is prevented by the chelating effect. The other approach method is the "principle of steric shielding".[19] Herein, bulky substituents (e.g. mesityl-groups) are attached to the boron, which leads to kinetic protection.[20] To not extend the π-system and to prevent changes to the molecular structure, we chose the method of steric shielding to stabilize the diazadiboraacene in our design.

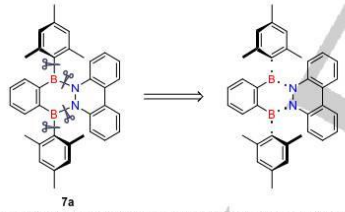

Scheme 1. Cut of the diazadiborabenzo[*b*]triphenylene **7a** in three synthetic parts.

We planned the synthesis of the mesitylated diazadibora benzo[*b*]triphenylene **7a** by firstly cutting the molecule in three synthetic parts: the diazine, the mesitylene and the boron backbone (Scheme 1). For the diazine moiety we relied on the benzo[*c*]cinnoline (**15**), which is commercially available and has been crucial in the preparation of the radical **16**. In contrast, the mesitylene part and the boron backbone have to be synthesized (Scheme 2).

For the boron backbone we chose the bis-BCl_2-benzene **10** as intermediate. Therefore, 1,2-dibromobenzene (**8**) was transformed in a Grignard reaction with Mg and TMSCl to the bis-TMS-benzene **9** in a yield of 34% (Scheme 2).[21] For the next step, we prepared a solution of bis-TMS-benzene **9** in dry DCM under Schlenk conditions in a pressure tube. The solution was cooled down to 0 °C and treated with 1 M solution of BCl_3 in DCM, sealed and heated to 95 °C for five days.[22] After removing the solvent and distillation of the crude bis-BCl_2-benzene **10** was obtained in 53%. For the mesitylene part, copper mesitylene **12** was chosen due to its selectivity for mono-substitution on boron atoms. Compound **12** was synthesized from bromomesitylene **11** by forming the Grignard reagent *in situ* followed by quenching with CuCl in THF solution. This provided the copper mesitylene **12** was accessed in a yield of 31%.[23] In the next step, the boron backbone was combined with the mesitylene part by adding the bis-BCl_2-benzene **10** to the copper mesitylene **12** in a toluene solution. After purification, the mesitylated bis-BCl-benzene **13** was isolated in a good yield of 71%. In the last step, the benzo[*c*]cinnoline (**15**) should be added to the mesitylated bis-BCl-benzene **13** to first form the corresponding Lewis adduct and ideally after a reduction the mesitylated diazadiborabenzo[*b*]triphenylene **7a** should be obtained. Therefore, the mesitylated bis-BCl-benzene **13** and benzo[*c*]cinnoline (**15**) were stirred in THF at room temperature for 12 h. Then, KC_8 was used as reducing agent. However, the desired product **7a** was not observed.[24] In addition, the transformation was attempted with Lewis acids e.g. $AlCl_3$ but this was unsuccessful,[25] probably due to steric reasons. In an attempt to circumvent this problem, we tried to replace the chloride on the boron by a hydride using $LiAlH_4$.[26] The salt was filtered off and benzo[*c*]cinnoline (**15**) was added to the filtrate. Additionally, TMSCl was added to this reaction mixture to form the corresponding borane *in situ*. Unfortunately, in this altered approach the desired product was also not observed. Only the starting materials could be re-isolated.

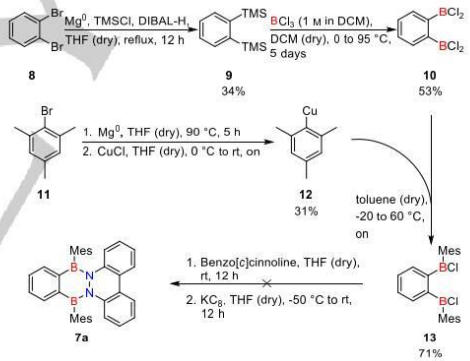

Scheme 2. Unsuccessful synthetic attempt to obtain the mesitylated diazadibora benzo[*b*]triphenylene **7a**.

As our initial strategy was not successful, we planned to establish the B−N connection of the molecule first and stabilize the scaffold afterwards by addition of the mesitylene component. We envisioned to exploit the equilibrium between the biradical **16** and **17** with respect to the coordination of a second benzo[*c*]cinnoline (**15**) (Scheme 3).[17] The synthesis commences with the preparation of lithium *o*-phenylbisborate **14** from the 1,2-dibromobenzene (**8**) via 1,2-bis(pinacolboryl)benzene according to the literature.[26] By treating the solution of lithium *o*-phenylbisborate **14** and benzo[*c*]cinnoline (**15**) with TMSCl the biradical **16** was formed, which is indicated by a dark green color. Then, the reaction mixture was treated with the mesityl Grignard reagent **18a** to capture the diazadibora unit from the equilibrium. This strategy was successful and provided the desired mesitylated diazadiborabenzo[*b*]triphenylene **7a**. During this

Angewandte Chemie International Edition 10.1002/anie.202300785

WILEY-VCH

COMMUNICATION

procedure the colour of the mixture turned from dark green to dark red. After concentration, the crude product was extracted with toluene. By overlaying the yellow toluene extract with methanol, the mesitylated diazadiborabenzo[*b*]triphenylene **7a** crystallized overnight as a yellow solid in a yield of 23%. By ^{1}H NMR experiments we could show the diazadibora **7a** to be air-stable in a THF-d_8 solution over 24 h (see SI for details). With an efficient modular synthesis approach in handy, we set out to test the scope of the strategy in terms of boron substitution. Therefore, we explored different aryl Grignard reagents **18b-h** with the same reaction set up. In this way, we could synthesize diazadibora derivatives **7b-h**. Due to their air and moisture sensitivity, they could not be purified by precipitation from the solution with methanol. The reaction mixture was therefore concentrated and the impurities were sublimated out of the crude mixture. The remaining solid was extracted with DCM and the combined extracts were concentrated under reduced pressure. In this way, the diazadiborabenzo[*b*]triphenylenes **7b-h** were obtained as pale-yellow solids in yields of 22 – 37%. In a similar fashion the diaza part as well as the *o*-phenylbisborate can be altered to provide a comprehensive overview of this new class of extended B,N-PAHs, which will be part of future studies.

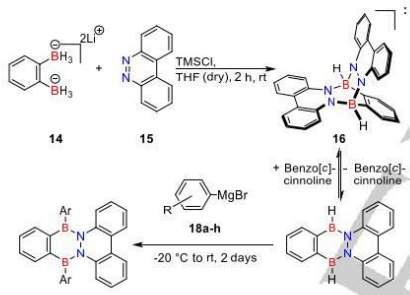

R =			
2,4,6-Trimethyl	**7a** (23%)	4-Methoxy	**7e** (23%)
2-Methyl	**7b** (37%)	4-Fluoro	**7f** (31%)
3-Methyl	**7c** (27%)	4-Chloro	**7g** (37%)
4-Methyl	**7d** (25%)	H	**7h** (22%)

Scheme 3. Synthesis of diazadiborabenzo[*b*]triphenylenes **7a-h**, starting from lithium *o*-phenylbisborate **14** and benzo[*c*]cinnoline (**15**).

The UV-Vis spectrum of **7a** (solid black line) is shown in comparison to the spectrum of the carbon analogue, benzo[*b*]triphenylene (**19**), (solid red line) in Figure 2 ($2.0 \cdot 10^{-5}$ M in DCM). One of the absorption maxima of **7a** is blue-shifted (λ_{max} = 248 nm) and the other maxima is red-shifted (λ_{max} = 350 nm) in comparison to the benzo[*b*]triphenylene (**19**) (λ_{max} = 277 & 289 nm). Additionally, we also investigated the absorption spectrum in THF and *n*-hexane, which resulted in very similar spectra (see SI for details). Hence, the polarity of the solvents has no significant influence on the absorption maxima of diazadibora **7a**. The UV-Vis spectra of the diazadibora derivatives **7b-h** are congruent with the spectra of **7a** (see SI for details). Furthermore, we also measured the emission spectra of **7a** (dotted black line) and for comparison also of the carbon analogue benzo[*b*]triphenylene (dotted red line). For the diazadibora **7a** we observed a red-shifted emission band ($\lambda_{em.}$ = 494 & 580 nm) after excitation at 350 nm in comparison to the carbon analog, exhibiting an unusual large Stokes shift of 144 (1.0 eV) and 230 nm (1.4 eV).

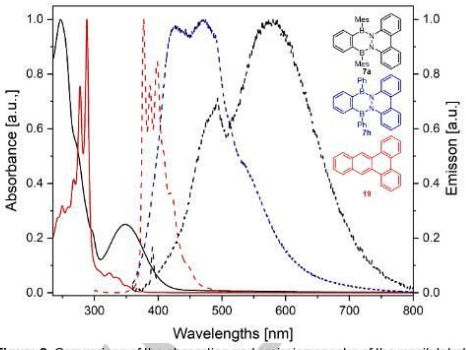

Figure 2. Comparison of the absorption and emission spectra of the mesitylated diazadiborabenzo[*b*]triphenylene **7a** and benzo[*b*]triphenylene (**19**). UV/Vis spectra of the mesitylated diazadiborabenzo[*b*]triphenylene **7a** (solid black line) and benzo[*b*]triphenylene (**19**) (solid red line) both in a concentration of $2.0 \cdot 10^{-5}$ M in DCM. The emission spectra of the diazadiborabenzo[b]triphenylene **7a** (dotted black line) and **7h** (dotted blue line) excited ar 350 nm in a concentration of $5.0 \cdot 10^{-4}$ M in DCM, and benzo[*b*]triphenylene (**19**) (dotted red line) excited at 277 nm ($2.5 \cdot 10^{-6}$ M in DCM).

The emission intensity of **7a** at 580 nm correlates linearly with the concentration range from $1.0 \cdot 10^{-5}$ to $5.0 \cdot 10^{-5}$ mol/L. However, at higher concentrations this relationship does not hold true (see SI for details) indicating concentration-dependent quenching. The unchanged emission profile at lower concentrations does not indicate excimer formation.[27] Furthermore, we also investigated the emission in different solvents with different polarities (see SI for details), such as THF, DCM, cyclohexane and *n*-hexane, and compared them at a concentration of $5.0 \cdot 10^{-5}$ mol/L and an excitation wavelength of 350 nm. The lowest emission intensity was observed in THF. With decreasing polarity of the solvent, the emission intensity increased with the highest emission observed in *n*-hexane. However, the wavelength of the emission maxima did not change with different solvent polarity. This observation indicates that the dipole moment within the molecules are relatively small due to competing effects of the B-N π-bonding and the difference in electronegativity. Also, the quantum yield was determined to be Φ_F = 0.3% for the diazadibora benzo[*b*]triphenylene **7a** in cyclohexane (see SI for details).

Table 1. Overview of the photophysical properties of **7a-h** excited at 300 and 350 nm in DCM, and the corresponding quantum yields of **7a-h** in cyclohexane.

Compound	Emission maxima ex. 300 nm [nm]	Emission maxima ex. 350 nm [nm]	Quantum Yield Φ_F [%]
7a	420, 490 & 560	494 & 580	0.3
7b	427	480	1.0
7c	328, 376 & 480	480	2.2
7d	340, 378 & 486	420	3.4
7e	381	478	4.2
7f	381	432	2.4
7g	416	441	8.1
7h	422	422 & 474	2.8

The diazadiboracompounds **7b-h** differ in their photophysical properties from **7a**. The results are summarized in Table 1. All spectra were measured at a concentration of $5.0 \cdot 10^{-4}$ mol/L in DCM and excited at 300 or 350 nm. Upon excitation with 350 nm,

Angewandte Chemie International Edition

10.1002/anie.202300785

WILEY-VCH

COMMUNICATION

the emission sprectra of **7b-h** exhibit maxima from 422 to 474 nm and only **7h** shows a dual emission band (Figure 2 – dotted blue line). Quantum yields between 1.0 and 8.1% in cyclohexane could be observed for **7b-h** (see SI for details), which are considerably higher than for **7a**. After excitation at 300 nm, the emission maxima of **7b-h** range from 328 to 480 nm. Additionally, **7c** & **7d** have three emission maxima. But none of them has a large Stokes shift as **7a**.

This observation could be due to the twisted $C_2B_2N_2$ core of **7a** (see crystal structure - Figure 3). The steric hinderance of the mesityl groups prevents the core of **7a** to be flat and may thus also inhibit the photochemical relaxation pathway. This is in agreement with the studies of Lu *et. al*. in 2019,[16] who showed that, the large Stokes shift is due to the twisting of the $C_2B_2N_2$ core in the diazadiboranapthalenes **6** in the excited state, which can be prevented in different matrices. Interestingly, our phosphorescence measurements showed a short-lived phosphorescence of all diazadiboratriphenyles **7a-h** between 12.5 and 15.0 msec (see SI for details). Additionally, the emission of **7a-h** can also be triggered with excitation wavelengths of 302 and 365 nm (see SI for details). Addionally, we monitored the emission processes of **7a-h** depending on exciation wavelengths of 300, 350, 380 and 400 nm. Herein, it could be shown that depending on the substitution on the boron-atom individual emission parthways are preffered with incresing excitation wavelengths (see SI for details).

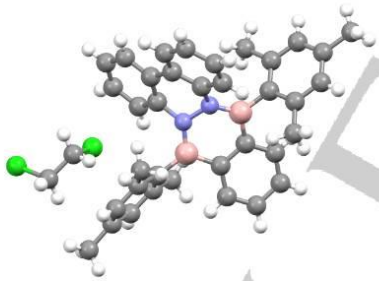

Figure 3. Experimental crystal structure of the diazadibora **7a** crystallized with 1,2-dichloroethane (CCDC- 2204514).

Quantum chemical calculations at the DFT/CAM-B3LYP level showed a good agreement between the computed ground-state equilibrium structure and the experimental crystal structure (Figure 3) with bond lengths varying by less than 0.01 Å and dihedral angles by less than 2°.[28] Subsequent calculations of the excited electronic states at TDDFT/CAM-B3LYP level yielded a computed UV/VIS spectrum (Figure 4), which also resembles the experimental one closely, albeit being blue shifted by approx. 0.5 eV due to missing solvation and vibronic effects.

The first peak of the UV-Vis spectrum consists of the first two singlet excited states S_1 (4.11 eV) and S_2 (4.29 eV). The corresponding detachment and attachment densities (Figure 5) characterize both as ππ* excitations, in which electron density is transferred from the central BN building block to the outer π systems of the central building block. The energetically lowest-lying triplet excited state T_1 has an excitation energy of 3.25 eV and corresponds to a ππ* excitation within the biphenylic building block of the central moiety (see Figure 5). Excitation energies and the corresponding detachment and attachment densities of energetically higher-lying states are given in the SI.

Further investigations showed a good agreement between the computed phosphorescence energy of 2.29 eV corresponding to an emission wavelength of 541 nm and λ_{max} of the experimental phosphorescence band at 575 nm. For this objective, the vertical decay energy has been computed at the equilibrium geometry of the T_1 state. To rationalize the occurrence of phosphorescence, possible intersystem crossing pathways from the singlet into the triplet state manifold need to be considered. According to Fermi's Golden rule, crossing rates are particularly high at points of state crossings, where the singlet and triplet states are energetically degenerate. Then ISC rates can be large despite small spin-orbit coupling elements.

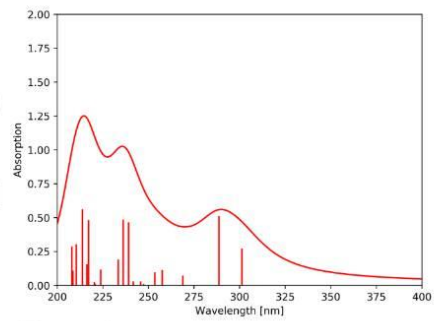

Figure 4. Computed UV/Vis absorption spectrum of the diazadiboraacene **7a**.

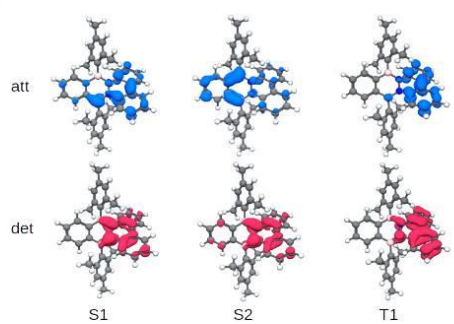

Figure 5. Detachment and attachment densities of the S_1, S_2 and T_1 of the diazadiboraacene **7a** at the ground-state equilibrium geometry.

Upon photoexcitation and internal conversion, the S_1 state is populated at the equilibrium geometry of the ground state, i.e. the Franck-Condon point on the S_1 surface. At this geometry, six triplet excited states are found to lie energetically below the S_1 state. During relaxation into its equilibrium geometry, the S_1 drops drastically in energy, and at the S1 equilibrium geometry only one

Angewandte Chemie International Edition 10.1002/anie.202300785

WILEY-VCH

COMMUNICATION

triplet state is found energetically lower than S_1 (Table 2). In other words, the PES of the S_1 crosses those of five triplet states during the initial relaxation. As described above, each of these singlet-triplet crossings allow in principle for ISC into the triplet manifold even though the spin-orbit coupling elements are small at TDDFT level computed at the Franck-Condon geometry as well as at the relaxed S_1 geometry. Once arrived in the triplet manifold, the molecules will continue to relax into the T_1 minimum and decay via the observed phosphorescence.

Table 2. Excitation energies for the lowest excited states of **7a** computed at the equilibrium geometries of the electronic ground state S_0, and the first excited singlet and triplet states S_1 and T_1, respectively.

S_0 eq. geometry		S_1 eq. geometry		T_1 eq. geometry	
State	ω [eV]	State	ω [eV]	State	ω [eV]
T_1	3.25	T_1	1.84	T_1	2.29
T_2	3.53	S_1	2.20	T_2	3.05
T_3	3.72	T_2	2.70	S_1	3.24
T_4	3.86	T_3	3.23	T_3	3.53
T_5	3.88	T_4	3.35	T_4	3.75
T_6	4.05	S_2	3.38	S_2	3.76
S_1	4.12	T_5	3.55	T_5	3.84
T_7	4.18	T_6	3.60	T_6	3.87
T_8	4.20	S_3	3.78	T_7	3.92
S_2	4.29	T_7	3.86	T_8	3.99

Additionally, the diazadiboratriphenylene **7a** was electrochemically characterized and cyclic voltammetry measurements in DCM showed an irreversible oxidation wave at + 1.31 (vs SCE). During CV measurements, no reduction wave was observed (see SI for details).

In summary, we presented a novel synthetic strategy to access diazadiborabenzo[*b*]triphenylene **7a-h** via biradical **16** as key intermediate. Thereby, we exploited the equilibrium of the coordination of the second benzo[*c*]cinnoline (**15**) of the biradical **16**. By addition of Grignard reagents **18a-h**, we were able to successfully access the diazadiborabenzo[*b*]triphenylene **7a-h**. We investigated the absorption, emission and excitation spectra of the novel diazadiboraacene **7a-h**. In contrast to diazadiboratriphenylene derivatives **5** from Jaska *et. al.*, which shows mainly a yellow-orange emission with maxima between 521 and 586 nm, we could show that the diazadiborabenzo[*b*]triphenylene **7a-h** have mainly a blue or green emission with maxima between 328 and 494 nm.[14] The quantum yields are in a similar range like those of diazadiboratriphenylene derivatives **5**. Only the quantum yield of **7a**, which has a similar emission maximum as **5**, has a lower quantum yield. In comparison with the azaboraanthracence **3**, which has an emission maximum of 447 nm, we could show that a larger dipole moment in the molecule does in general not lead to a larger Stokes shift.[12] We could demonstrate that small changes at the boron-attached aryl-ring can have a significant influence on the emission properties. Additionally, the emission could be assigned to short life-time phosphorescence. The exact relaxation of the different derivates **7a-h** will be investigated in future studies. In conclusion, we synthesized novel B,N benzo[*b*]triphenylenes with tunable emission properties via a highly modular synthetic route, giving access to a new class of B,N-PAHs with promising potential as molecular materials.

Acknowledgements

The authors thank the DFG for funding, Heike Hausmann (Justus Liebig University, Giessen) for NMR-measurements, Frederik R. Erb (Justus Liebig University, Giessen) for CV measurements and Michel Große (Justus Liebig University, Giessen) for X-Ray analysis.

Keywords: boron • nitrogen • polycycles • phosphorescence • acenes

[1] a) R. Freudenmann, B. Behnisch, M. Hanack, *J. Mater. Chem.* **2001**, *11*, 1618–1624; b) G. Albrecht, C. Geis, J. M. Herr, J. Ruhl, R. Göttlich, D. Schlettwein, *Org. Electron.* **2019**, *65*, 321–326; c) I. Seguy, P. Jolinat, P. Destruel, J. Farenc, R. Mamy, H. Bock, J. Ip, T. P. Nguyen, *J. Appl. Phys.* **2001**, *89*, 5442–5448.

[2] a) D. Adam, F. Closs, T. Frey, D. Funhoff, D. Haarer, P. Schuhmacher, K. Siemensmeyer, *Phys. Rev. Lett.* **1993**, *70*, 457–460; b) D. Adam, P. Schuhmacher, J. Simmerer, L. Häussling, K. Siemensmeyer, K. H. Etzbachi, H. Ringsdorf, D. Haarer, *Nature* **1994**, *371*, 141–143.

[3] M. Oukachmih, P. Destruel, I. Seguy, G. Ablart, P. Jolinat, S. Archambeau, M. Mabiala, S. Fouet, H. Bock, *Sol. Energy Mater. Sol. Cells* **2005**, *85*, 535–543.

[4] a) M. D. Watson, A. Fechtenkötter, K. Müllen, *Chem. Rev.* **2001**, *101*, 1267–1300; b) J. Wu, W. Pisula, K. Müllen, *Chem. Rev.* **2007**, *107*, 718–747; c) M. Bendikov, F. Wudl, D. F. Perepichka, *Chem. Rev.* **2004**, *104*, 4891–4946.

[5] P. G. Campbell, A. J. V. Marwitz, S.-Y. Liu, *Angew. Chem. Int. Ed.* **2012**, *51*, 6074–6092.

[6] a) C. Mützel, J. M. Farrell, K. Shoyama, F. Würthner, *Angew. Chem. Int. Ed.* **2022**, *61*, e202115746; b) Q. Shi, X. Shi, C. Feng, Y. Wu, N. Zheng, J. Liu, X. Wu, H. Chen, A. Peng, J. Li et al., *Angew. Chem. Int. Ed.* **2021**, *133*, 2960–2964; c) A. John, S. Kirschner, M. K. Fengel, M. Bolte, H.-W. Lerner, M. Wagner, *Dalton Trans.* **2019**, *48*, 1871–1877.

[7] a) Z. Liu, T. B. Marder, *Angew. Chem. Int. Ed.* **2008**, *47*, 242–244; b) T. Lorenz, M. Crumbach, T. Eckert, A. Lik, H. Helten, *Angew. Chem. Int. Ed.* **2017**, *56*, 2780–2784; c) X. Chen, D. Tan, D.-T. Yang, *J. Mater. Chem. C* **2022**, *10*, 13499–13532; d) H. Gotoh, S. Nakatsuka, H. Tanaka, N. Yasuda, Y. Haketa, H. Maeda, T. Hatakeyama, *Angew. Chem. Int. Ed.* **2021**, *133*, 12945–12950; e) T. Kaehler, M. Bolte, H.-W. Lerner, M. Wagner, *Angew. Chem. Int. Ed.* **2019**, *58*, 11379–11384; f) M. Krieg, F. Reicherter, P. Haiss, M. Ströbele, K. Eichele, M.-J. Treanor, R. Schaub, H. F. Bettinger, *Angew. Chem. Int. Ed.* **2015**, *54*, 8284–8286; g) M. Müller, S. Behnle, C. Maichle-Mössmer, H. F. Bettinger, *Chem. Commun.* **2014**, *50*, 7821–7823; h) G. Bélanger - Chabot, H. Braunschweig, D. K. Roy, *Eur. J. Inorg. Chem.* **2017**, *2017*, 4353–4368; i) A. Maiti, B. J. Elvers, S. Bera, F. Lindl, I. Krummenacher, P. Ghosh, H. Braunschweig, C. B. Yildiz, C. Schulzke, A. Jana, *Chem. Eur. J.* **2022**, *28*, e202104567; j) A. S. Scholz, J. G. Massoth, M. Bursch, J.-M. Mewes, T. Hetzke, B. Wolf, M. Bolte, H.-W. Lerner, S. Grimme, M. Wagner, *J. Am. Chem. Soc.* **2020**, *142*, 11072–11083; k) M. R. Rapp, W. Leis, F. Zinna, L. Di Bari, T. Arnold, B. Speiser, M. Seitz, H. F. Bettinger, *Chem. Eur. J.* **2022**, *28*, e202104161; l) M. Fingerle, C. Maichle-Mössmer, S. Schundelmeier, B. Speiser, H. F. Bettinger, *Org. Lett.* **2017**, *19*, 4428–4431; m) M. Stępień, E. Gońka, M. Żyła, N. Sprutta, *Chem. Rev.* **2017**, *117*, 3479–3716.

[8] M. J. S. Dewar, V. P. Kubba, R. Pettit, *J. Chem. Soc.* **1958**, 3073–3076.

[9] a) M. J. S. Dewar, R. Dietz, *J. Org. Chem.* **1961**, *26*, 3253–3256; b) S. S. Chissick, M. Dewar, P. M. Maitlis, *Tetrahedron Lett.* **1960**, *1*, 8–10; c) F. A. Davis, M. Dewar, R. Jones, S. D. Worley, *J. Am. Chem. Soc.* **1969**, *91*, 2094–2097; d) M. J. S. Dewar, P. M. Maitlis, *J. Am. Chem. Soc.* **1961**, *83*, 187–193; e) M. Dewar, V. P. Kubba, *Tetrahedron* **1959**, *7*, 213–222; f) M. Dewar, R. Jones, *J. Am. Chem. Soc.* **1968**, *90*, 2137–2144; g) M. Dewar, R. Dietz, V. P. Kubba, A. R. Lepley, *J. Am. Chem. Soc.* **1961**, *83*, 1754–1756; h) M. Dewar, G. J. Gleicher, B. P. Robinson, *J. Am. Chem. Soc.* **1964**, *86*, 5698–5699; i) M. Dewar, V. P. Kubba, *J. Am. Chem. Soc.* **1961**, *83*, 1757–1760.

[10] a) T. Hasegawa, J. Takeya, *Sci. Technol. Adv. Mater.* **2009**, *10*, 024314; b) T. Hatakeyama, S. Hashimoto, S. Seki, M. Nakamura, *J. Am. Chem. Soc.* **2011**, *133*, 18614–18617; c) J. E. Anthony, *Chem. Rev.* **2006**, *106*, 5028–5048; d) J. E. Anthony, *Angew. Chem. Int. Ed.* **2008**, *47*, 452–483; e) M. J. D. Bosdet, W. E. Piers, T. S. Sorensen, M. Parvez, *Angew. Chem. Int. Ed.* **2007**, *46*, 4940–4943.

Angewandte Chemie International Edition

10.1002/anie.202300785

WILEY-VCH

COMMUNICATION

[11] J. S. A. Ishibashi, J. L. Marshall, A. Mazière, G. J. Lovinger, B. Li, L. N. Zakharov, A. Dargelos, A. Graciaa, A. Chrostowska, S.-Y. Liu, *J. Am. Chem. Soc.* **2014**, *136*, 15414–15421.
[12] D. Tian, G. Shi, M. Fan, X. Guo, Y. Yuan, S. Wu, J. Liu, J. Zhang, S. Xing, B. Zhu, *Org. Lett.* **2021**, *23*, 8163–8168.
[13] a) W. Siebert, R. Full, H. Schmidt, J. von Seyerl, M. Halstenberg, G. Huttner, *J. Organomet. Chem.* **1980**, *191*, 15–25; b) H. Schmidt, W. Siebert, *J. Organomet. Chem.* **1978**, *155*, 157–163.
[14] C. A. Jaska, D. J. H. Emslie, M. J. D. Bosdet, W. E. Piers, T. S. Sorensen, M. Parvez, *J. Am. Chem. Soc.* **2006**, *128*, 10885–10896.
[15] M. J. Bosdet, W. E. Piers, T. S. Sorensen, M. Parvez, *Can. J. Chem.* **2010**, *88*, 426–433.
[16] Z. Lu, H. Quanz, J. Ruhl, G. Albrecht, C. Logemann, D. Schlettwein, P. R. Schreiner, H. A. Wegner, *Angew. Chem. Int. Ed.* **2019**, *58*, 4259–4263.
[17] Z. Lu, H. Quanz, O. Burghaus, J. Hofmann, C. Logemann, S. Beeck, P. R. Schreiner, H. A. Wegner, *J. Am. Chem. Soc.* **2017**, *139*, 18488–18491.
[18] Z. Zhou, A. Wakamiya, T. Kushida, S. Yamaguchi, *J. Am. Chem. Soc.* **2012**, *134*, 4529–4532.
[19] a) C. Reus, S. Weidlich, M. Bolte, H.-W. Lerner, M. Wagner, *J. Am. Chem. Soc.* **2013**, *135*, 12892–12907; b) T. Agou, M. Sekine, T. Kawashima, *Tetrahedron Lett.* **2010**, *51*, 5013–5015.
[20] V. M. Hertz, N. Ando, M. Hirai, M. Bolte, H.-W. Lerner, S. Yamaguchi, M. Wagner, *Organometallics* **2017**, *36*, 2512–2519.
[21] a) H. F. Bettinger, M. Filthaus, *J. Org. Chem.* **2007**, *72*, 9750–9752; b) D. Kaufmann, *Chem. Ber.* **1987**, *120*, 901–905.
[22] S. Bader, S. Kessler, H. Wegner, *Synthesis* **2010**, *2010*, 2759–2762.
[23] a) H. Eriksson, M. Håkansson, *Organometallics* **1997**, *16*, 4243–4244; b) M. Schlosser, V. Ladenberger, *J. Organometal. Chem.* **1967**, *8*, 193–197; c) G. Costa, A. Camus, L. Gatti, N. Marsich, *J. Organometal. Chem.* **1966**, *5*, 568–572.
[24] a) Di Wu, L. Kong, Y. Li, R. Ganguly, R. Kinjo, *Nat. Commun.* **2015**, *6*, 7340; b) M.-A. Légaré, G. Bélanger-Chabot, R. D. Dewhurst, E. Welz, I. Krummenacher, B. Engels, H. Braunschweig, *Science* **2018**, *359*, 896–900; c) B. Wang, Y. Li, R. Ganguly, H. Hirao, R. Kinjo, *Nat. Commun.* **2016**, *7*, 11871.
[25] a) C. K. Narula, H. Noeth, *Inorg. Chem.* **1985**, *24*, 2532–2539; b) U. Höbel, H. Nöth, H. Prigge, *Chem. Ber.* **1986**, *119*, 325–337.
[26] Ö. Seven, Z.-W. Qu, H. Zhu, M. Bolte, H.-W. Lerner, M. C. Holthausen, M. Wagner, *Chem. Eur. J.* **2012**, *18*, 11284–11295.
[27] H. Saigusa, E. C. Lim, *Acc. Chem. Res.* **1996**, *29*, 171–178.
[28] T. Yanai, D. P. Tew, N. C. Handy, *Chem. Phys. Lett.* **2004**, *393*, 51–57.

3. Additional Contribution to Literature

Mechanistic Study of Domino Processes Involving the Bidentate Lewis Acid Catalyzed Inverse Electron-Demand Diels−Alder Reaction

“The detailed understanding of mechanisms is the basis to design new reactions. Herein, we studied the domino bidentate Lewis acid catalyzed inverse electron-demand Diels−Alder (IEDDA) reaction developed in our laboratory computationally as well as by synthetic experiments, to characterize different pathways. A quinodimethane intermediate was identified as key structure, which is the basis for all subsequent transformations: Elimination to an aromatic naphthalene, rearrangement to a dihydroaminonaphthalene and a photo-induced ring opening. These insights allow to optimize the reaction conditions, such as catalytic utilization of amine, as well as to advance new reactions in the future.”

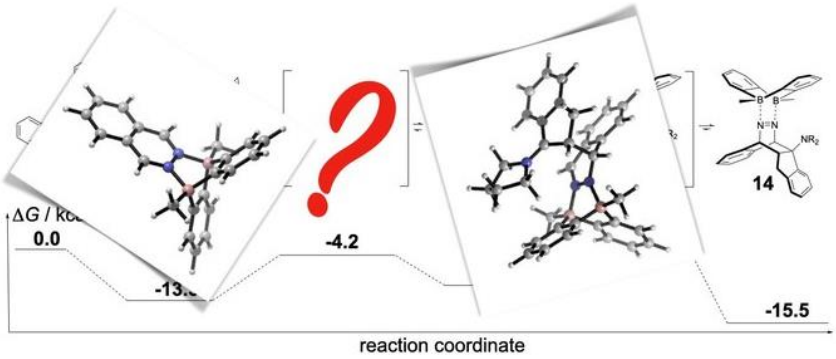

Reference:

Marcel A. Strauss, Daniel Kohrs, Julia Ruhl, Hermann A. Wegner, *Eur. J. Org. Chem.* **2021**, *28*, 3866-3873. DOI: 10.1002/ejoc.202100486

4. Acknowledgement/Danksagung

Als Erstes möchte ich mich bei Prof. Dr. Hermann A. Wegner für die Möglichkeit meine Doktorarbeit in seiner Arbeitsgruppe anzufertigen, seine Unterstützung, sowie sein Vertrauen in mich zu bedanken.

Für die Begutachtung und das Anfertigen eines Zweitgutachtens möchte ich bei Prof. Dr. Richard Göttlich bedanken.

Das größte Dankeschön geht an Georg, der mich immer unterstützt und nach so manchen Rückschlägen im Labor wieder aufgebaut hat. Und natürlich auch an meine Eltern, meine Großmütter und meinen Bruder, die immer mit großer Unterstützung für mich da waren. Ohne euch wäre mein ganzes Studium nicht möglich gewesen.

Ein riesiges Dankeschön geht an meine beste Freundin Mimi und ihren fast Ehemann Kevin, die mittlerweile eher Familie statt Freunde sind. Ihr wart immer für mich da, auch wenn ihr nicht zu genau Wissen wolltet, was ich da eigentlich mache.

Weiterhin möchte ich mich bei Dr. Sebastian Ahles und Dr. Marcel A. Strauss, für alles was sie mir seit dem Bachelor beigebracht haben, bedanken. Aber natürlich auch für alle schönen Momente innerhalb und außerhalb der Arbeitsgruppe.

Ein sehr großer Dank geht an Daniel Kohrs und Mari Janse van Rensburg, die mir nicht nur an der Arbeit immer zur Seite standen, sondern auch über die Jahre zu sehr guten Freunden wurden.

Natürlich möchte ich mich auch bei der gesamten Arbeitsgruppe Wegner für die tollen Jahre bedanken. Hier möchte ich mich im Besonderen nochmal bei Christopher M. Leonhardt, Dr. Anne Kunz, Katinka Grimmeisen, Conrad Averdunk, Kai Hanke, Michel Große, Dominic Schatz, Finn Schneider, Jannis Volkmann, Felix Berndt, Dr. Andreas H. Heindl, Sebastian Beeck, Dr. Longcheng Hong, Jan H. Griwatz, Saskia Lehr, Nathaniel Ukah und Niklas Koch für die lustigen und schönen Momente im Labor und beim ein oder anderen Bier bedanken. Außerdem für die schönen Gruppenausflüge, die mir immer sehr viel Spaß gemacht haben.

Des Weiteren möchte ich mich bei meiner ehemaligen Kommilitonin und jetzt sehr lieben Freundin Dr. Melanie Sieland für all die schönen Momente und die Unterstützung in den letzten Jahren bedanken.

Ich möchte mich auch bei unseren tollen Sekretärinnen Anika Jäger und Michaela Richter für ihre Unterstützung bedanken.

Keine Doktorarbeit kommt ohne die Hilfe der technischen und administrativen Mitarbeiter aus, die mit ihrer Unterstützung unsere Forschung sehr stark weiter bringen. Daher gebührt auch ein ganz großer Dank Dr. Dennis Gerbig, Dr. Rafael Wende. Dr. Heike Hausmann, Dr. Jörg Neudert, Anika Bernhardt, Anja Platt, Ina Klein, Brigitte Weinl-Boulakhrouf, Eike Santoswski, Mario Dauber, Steffen Wagner, Stefan Berndardt und an unsere liebe Anja Beneckstein.

5. Abbreviations

Abs.	Absorption
BDE	Bond dissociation energy
BDLA	Bidentate Lewis acid
DA	Diels-Alder
DCM	Dichloromethane
EDG	Electron donating group
Em.	Emission
EWG	Electron withdrawing group
h	Hours
HOMO	Highest occupied molecular orbital
IEDDA	Inverse electron demand Diels-Alder
LA	Lewis acid
LDA	Lithium diisopropylamide
LED	Light emitting diode
LUMO	Lowest unoccupied molecular orbital
min	Minutes
OFETs	Organic field-effect transistors
OLEDs	Organic light-emitting diodes
PAHs	Polycyclic aromatic hydrocarbons
PIRO	Photoinduced ring-opening
rt	Room temperature
THF	Tetrahydrofuran
TICT	Twisted intramolecular charge transfer

6. References

[1] P. G. Campbell, A. J. V. Marwitz, S.-Y. Liu, *Angew. Chem. Int. Ed.* **2012**, *51*, 6074–6092.

[2] Z. Liu, T. B. Marder, *Angew. Chem. Int. Ed.* **2008**, *47*, 242–244.

[3] a) A. Suzuki, *Angew. Chem. Int. Ed.* **2011**, *50*, 6722–6737; b) R. M. Washburn, *Inorg. Chem.* **1963**, *2*, p. 884; c) H. C. Brown, C. G. Scouten, K. K. Wang, *J. Org. Chem.* **1979**, *44*, 2589–2591; d) H. C. Brown, C. G. Scouten, R. Liotta, *J. Am. Chem. Soc.* **1979**, *101*, 96–99.

[4] R. H. Pritchard, C. W. Kern, *J. Am. Chem. Soc.* **1969**, *91*, 1631–1635.

[5] S. J. Blanksby, G. B. Ellison, *Acc. Chem. Res.* **2003**, *36*, 255–263.

[6] L. R. Thorne, R. D. Suenram, F. J. Lovas, *J. Chem. Phys.* **1983**, *78*, 167–171.

[7] D. J. Grant, D. A. Dixon, *J. Phys. Chem. A* **2006**, *110*, 12955–12962.

[8] A. Stock, E. Pohland, *Ber. dtsch. Chem. Ges. A/B* **1926**, *59*, 2210–2215.

[9] a) Y. Sato, M. Yato, T. Ohwada, S. Saito, K. Shudo, *J. Am. Chem. Soc.* **1995**, *117*, 3037–3043; b) K. Hattori, H. Yamamoto, *J. Org. Chem.* **1992**, *57*, 3264–3265; c) V. Nori, F. Pesciaioli, A. Sinibaldi, G. Giorgianni, A. Carlone, *Catalysts* **2022**, *12*, 5–27; d) T. Sugasawa, T. Toyoda, M. Adachi, K. Sasakura, *J. Am. Chem. Soc.* **1978**, *100*, 4842–4852; e) G. A. Olah, S. Kobayashi, M. Tashiro, *J. Am. Chem. Soc.* **1972**, *94*, 7448–7461.

[10] Y. S. Cheng, E. Ho, P. S. Mariano, H. L. Ammon, *J. Org. Chem.* **1985**, *50*, 5678–5686.

[11] H. v. Euler, K. O. Josephson, *Ber. dtsch. Chem. Ges. A/B* **1920**, *53*, 822–826.

[12] a) O. Diels, K. Alder, *Justus Liebigs Ann. Chem.* **1928**, *460*, 98–122; b) O. Diels, K. Alder, *Justus Liebigs Ann. Chem.* **1929**, *470*, 62–103.

[13] K. C. Nicolaou, S. A. Snyder, T. Montagnon, G. Vassilikogiannakis, *Angew. Chem. Int. Ed.* **2002**, *41*, 1668–1698.

[14] G. J. Bodwell, J. Li, *Angew. Chem. Int. Ed.* **2002**, *41*, 3261–3262.

[15] J. Sauer, R. Sustmann, *Angew. Chem. Int. Ed.* **1980**, *19*, 779–807.

[16] R. B. Woodward, R. Hoffmann, *Angew. Chem. Int. Ed.* **1969**, *8*, 781–853.

[17] a) D. Kato, Y. Sasaki, D. L. Boger, *J. Am. Chem. Soc.* **2010**, *132*, 3685–3687; b) Y. Murata, N. Kato, K. Komatsu, *J. Org. Chem.* **2001**, *66*, 7235–7239.

[18] a) Z. Zhu, D. L. Boger, *J. Org. Chem.* **2022**, *87*, 14657–14672; b) Y.-F. Yang, Y. Liang, F. Liu, K. N. Houk, *J. Am. Chem. Soc.* **2016**, *138*, 1660–1667.

[19] D. L. Boger, J. S. Panek, *J. Org. Chem.* **1983**, *48*, 621–623.

[20] D. L. Boger, R. F. Menezes, T. Honda, *Angew. Chem. Int. Ed.* **1993**, *32*, 273–275.

[21] a) H. Ishikawa, G. I. Elliott, J. Velcicky, Y. Choi, D. L. Boger, *J. Am. Chem. Soc.* **2006**, *128*, 10596–10612; b) J. E. Sears, T. J. Barker, D. L. Boger, *Org. Lett.* **2015**, *17*, 5460–5463.

[22] C. M. Glinkerman, D. L. Boger, *J. Am. Chem. Soc.* **2016**, *138*, 12408–12413.

[23] L. S. Povarov, B. M. Mikhailov, *Izv. Akad. Nauk SSSR, Ser. Khim.* **1964**, *13*, 2121–2122.

[24] a) P. H. Daniels, J. L. Wong, J. L. Atwood, L. G. Canada, R. D. Rogers, *J. Org. Chem.* **1980**, *45*, 435–440; b) O. Tsuge, S. Kanemasa, K. Matsuda, *J. Org. Chem.* **1984**, *49*, 2688–2691; c) M. E. Jung, J. J. Shapiro, *J. Am. Chem. Soc.* **1980**, *102*, 7862–7866.

[25] a) T. Ooi, T. Miura, K. Maruoka, *Angew. Chem. Int. Ed.* **1998**, *37*, 2347–2349; b) H. Li, T. J. Marks, *Proc. Natl. Acad. Sci. U.S.A.* **2006**, *103*, 15295–15302; c) K. Maruoka, *Catal. Today* **2001**, *66*, 33–45.

[26] A. Lorbach, M. Bolte, H.-W. Lerner, M. Wagner, *Chem. Commun.* **2010**, *46*, 3592–3594.

[27] C. A. Jaska, D. J. H. Emslie, M. J. D. Bosdet, W. E. Piers, T. S. Sorensen, M. Parvez, *J. Am. Chem. Soc.* **2006**, *128*, 10885–10896.

[28] F. P. Gabbaï, A. Schier, J. Riede, M. J. Hynes, *Chem. Commun.* **1998**, 897–898.

[29] H. Schulz, H. Pritzkow, W. Siebert, *Chem. Ber.* **1991**, *124*, 2203–2207.

[30] a) W. Schacht, D. Kaufmann, *J. Organomet. Chem.* **1987**, *331*, 139–152; b) W. E. Piers, G. J. Irvine, V. C. Williams, *Eur. J. Inorg. Chem.* **2000**, *2000*, 2131–2142.

[31] S. N. Kessler, H. A. Wegner, *Org. Lett.* **2010**, *12*, 4062–4065.

[32] S. N. Kessler, M. Neuburger, H. A. Wegner, *Eur. J. Org. Chem.* **2011**, *2011*, 3238–3245.

[33] S. Bader, S. Kessler, H. Wegner, *Synthesis* **2010**, *2010*, 2759–2762.

[34] Ö. Seven, M. Bolte, H.-W. Lerner, M. Wagner, *Organometallics* **2014**, *33*, 1291–1299.

[35] L. Hong, S. Ahles, A. H. Heindl, G. Tiétcha, A. Petrov, Z. Lu, C. Logemann, H. A. Wegner, *Beilstein J. Org. Chem.* **2018**, *14*, 618–625.

[36] S. N. Kessler, *Doctoral thesis, University of Basel* **2013**.

[37] a) T. H. Dunning, *J. Chem. Phys.* **1989**, *90*, 1007–1023; b) A. D. Becke, *J. Chem. Phys.* **1993**, *98*, 5648–5652; c) C. Lee, W. Yang, R. G. Parr, *Phys. Rev. B* **1988**, *37*, 785–789.

[38] L. Schweighauser, I. Bodoky, S. Kessler, D. Häussinger, H. Wegner, *Synthesis* **2012**, *44*, 2195–2199.

[39] L. Schweighauser, I. Bodoky, S. N. Kessler, D. Häussinger, C. Donsbach, H. A. Wegner, *Org. Lett.* **2016**, *18*, 1330–1333.

[40] L. Schweighauser, H. A. Wegner, *Chem. Eur. J.* **2016**, *22*, 14094–14103.

[41] S. Ahles, J. Ruhl, M. A. Strauss, H. A. Wegner, *Org. Lett.* **2019**, *21*, 3927–3930.

[42] S. Beeck, S. Ahles, H. A. Wegner, *Chem. Eur. J.* **2022**, *28*, e202104085.

[43] S. Ahles, S. Götz, L. Schweighauser, M. Brodsky, S. N. Kessler, A. H. Heindl, H. A. Wegner, *Org. Lett.* **2018**, *20*, 7034–7038.

[44] S. N. Kessler, M. Neuburger, H. A. Wegner, *J. Am. Chem. Soc.* **2012**, *134*, 17885–17888.

[45] S. N. Kessler, H. A. Wegner, *Org. Lett.* **2012**, *14*, 3268–3271.

[46] H. Wegner, S. Kessler, *Synlett* **2012**, *23*, 699–705.

[47] a) D. Adam, F. Closs, T. Frey, D. Funhoff, D. Haarer, P. Schuhmacher, K. Siemensmeyer, *Phys. Rev. Lett.* **1993**, *70*, 457–460; b) D. Adam, P. Schuhmacher, J. Simmerer, L. Häussling, K. Siemensmeyer, K. H. Etzbachi, H. Ringsdorf, D. Haarer, *Nature* **1994**, *371*, 141–143; c) J. E. Anthony, *Angew. Chem. Int. Ed.* **2008**, *47*, 452–483.

[48] a) R. Freudenmann, B. Behnisch, M. Hanack, *J. Mater. Chem.* **2001**, *11*, 1618–1624; b) I. Seguy, P. Jolinat, P. Destruel, J. Farenc, R. Mamy, H. Bock, J. Ip, T. P. Nguyen, *J. Appl. Phys.* **2001**, *89*, 5442–5448.

[49] M. Oukachmih, P. Destruel, I. Seguy, G. Ablart, P. Jolinat, S. Archambeau, M. Mabiala, S. Fouet, H. Bock, *Sol. Energy Mater. Sol.* **2005**, *85*, 535–543.

[50] a) M. Bendikov, F. Wudl, D. F. Perepichka, *Chem. Rev.* **2004**, *104*, 4891–4946; b) M. D. Watson, A. Fechtenkötter, K. Müllen, *Chem. Rev.* **2001**, *101*, 1267–1300; c) J. Wu, W. Pisula, K. Müllen, *Chem. Rev.* **2007**, *107*, 718–747.

[51] a) E. von Grotthuss, A. John, T. Kaese, M. Wagner, *Asian J. Org. Chem.* **2018**, *7*, 37–53; b) C. Mützel, J. M. Farrell, K. Shoyama, F. Würthner, *Angew. Chem. Int. Ed.* **2022**, *61*, e202115746; c) A. John, S. Kirschner, M. K. Fengel, M. Bolte, H.-W. Lerner, M. Wagner, *Dalton Trans.* **2019**, *48*, 1871–1877.

[52] a) T. Lorenz, M. Crumbach, T. Eckert, A. Lik, H. Helten, *Angew. Chem. Int. Ed.* **2017**, *56*, 2780–2784; b) X. Chen, D. Tan, D.-T. Yang, *J. Mater. Chem. C* **2022**, *10*, 13499–13532; c) H. Gotoh, S. Nakatsuka, H. Tanaka, N. Yasuda, Y. Haketa, H. Maeda, T. Hatakeyama, *Angew. Chem. Int. Ed.* **2021**, *133*, 12945–12950; d) T. Kaehler, M. Bolte, H.-W. Lerner, M. Wagner, *Angew. Chem. Int. Ed.* **2019**, *58*, 11379–11384; e) M. Krieg, F. Reicherter, P. Haiss, M. Ströbele, K. Eichele, M.-J. Treanor, R. Schaub, H. F. Bettinger, *Angew. Chem. Int. Ed.* **2015**, *54*, 8284–8286; f) M. Müller, S. Behnle, C. Maichle-Mössmer, H. F. Bettinger, *Chem. Commun.* **2014**, *50*, 7821–7823; g) M. R. Rapp, W. Leis, F. Zinna, L. Di Bari, T. Arnold, B. Speiser, M. Seitz, H. F. Bettinger, *Chem. Eur. J.* **2022**, *28*, e202104161; h) A. S. Scholz, J. G. Massoth, M. Bursch, J.-M. Mewes, T. Hetzke, B. Wolf, M. Bolte, H.-W. Lerner, S. Grimme, M. Wagner, *J. Am. Chem. Soc.* **2020**, *142*, 11072–11083.

[53] M. J. S. Dewar, R. Dietz, *J. Chem. Soc.* **1959**, 2728–2730.

[54] M. J. S. Dewar, V. P. Kubba, R. Pettit, *J. Chem. Soc.* **1958**, 3073–3076.

[55] M. J. S. Dewar, R. Dietz, *J. Org. Chem.* **1961**, *26*, 3253–3256.

[56] S. S. Chissick, M. Dewar, P. M. Maitlis, *Tetrahedron Lett.* **1960**, *1*, 8–10.

[57] a) M. Dewar, R. Jones, *J. Am. Chem. Soc.* **1968**, *90*, 2137–2144; b) M. J. S. Dewar, R. Dietz, V. P. Kubba, A. R. Lepley, *J. Am. Chem. Soc.* **1961**, *83*, 1754–1756; c) M. J. S. Dewar, G. J. Gleicher, B. P. Robinson, *J. Am. Chem. Soc.* **1964**, *86*, 5698–5699; d) M. J. S. Dewar, V. P. Kubba, *J. Am. Chem. Soc.* **1961**, *83*, 1757–1760.

[58] M. J. D. Bosdet, W. E. Piers, T. S. Sorensen, M. Parvez, *Angew. Chem. Int. Ed.* **2007**, *46*, 4940–4943.

[59] T. Hatakeyama, S. Hashimoto, S. Seki, M. Nakamura, *J. Am. Chem. Soc.* **2011**, *133*, 18614–18617.

[60] a) P. J. Grisdale, J. L. R. Williams, *J. Org. Chem.* **1969**, *34*, 1675–1677; b) P. Grisdale, M. Glogowski, J. L. R. Williams, *J. Org. Chem.* **1971**, *36*, 3821–3824; c) M. E. Glogowski, J. Williams, *J. Organomet. Chem.* **1980**, *195*, 123–135; d) M. E.

Glogowski, P. J. Grisdale, J. Williams, T. H. Regan, *J. Organomet. Chem.* **1973**, *54*, 51–60.

[61] M. J. D. Bosdet, C. A. Jaska, W. E. Piers, T. S. Sorensen, M. Parvez, *Org. Lett.* **2007**, *9*, 1395–1398.

[62] V. Mamane, P. Hannen, A. Fürstner, *Chem. Eur. J.* **2004**, *10*, 4556–4575.

[63] a) H. Tian, J. Shi, S. Dong, D. Yan, L. Wang, Y. Geng, F. Wang, *Chem. Commun.* **2006**, 3498–3500; b) H. Tian, J. Wang, J. Shi, D. Yan, L. Wang, Y. Geng, F. Wang, *J. Mater. Chem.* **2005**, *15*, 3026–3033.

[64] Z. Zhou, A. Wakamiya, T. Kushida, S. Yamaguchi, *J. Am. Chem. Soc.* **2012**, *134*, 4529–4532.

[65] a) C. Reus, S. Weidlich, M. Bolte, H.-W. Lerner, M. Wagner, *J. Am. Chem. Soc.* **2013**, *135*, 12892–12907; b) T. Agou, M. Sekine, T. Kawashima, *Tetrahedron Lett.* **2010**, *51*, 5013–5015.

[66] H. Maeda, T. Maeda, K. Mizuno, K. Fujimoto, H. Shimizu, M. Inouye, *Chem. Eur. J.* **2006**, *12*, 824–831.

[67] B. Asgarouladi, R. Full, K.-J. Schaper, W. Siebert, *Chem. Ber.* **1974**, *107*, 34–47.

[68] W. Siebert, R. Full, J. Edwin, K. Kinberger, *Chem. Ber.* **1978**, *111*, 823–831.

[69] W. Siebert, R. Full, H. Schmidt, J. von Seyerl, M. Halstenberg, G. Huttner, *J. Organomet. Chem.* **1980**, *191*, 15–25.

[70] H. Schmidt, W. Siebert, *J. Organomet. Chem.* **1978**, *155*, 157–163.

[71] D. J. H. Emslie, W. E. Piers, M. Parvez, *Angew. Chem. Int. Ed.* **2003**, *42*, 1252–1255.

[72] I. Ghesner, W. E. Piers, M. Parvez, R. McDonald, *Organometallics* **2004**, *23*, 3085–3087.

[73] T. Tanikawa, M. Saito, J. D. Guo, S. Nagase, *Org. Biomol. Chem.* **2011**, *9*, 1731–1735.

[74] I. B. Berlman (Ed.) *Handbook of fluorescence spectra of aromatic molecules* (Second Edition), Academic Press, New York City, NY, **1971**.

[75] Z. Lu, H. Quanz, J. Ruhl, G. Albrecht, C. Logemann, D. Schlettwein, P. R. Schreiner, H. A. Wegner, *Angew. Chem. Int. Ed.* **2019**, *58*, 4259–4263.

[76] Ö. Seven, Z.-W. Qu, H. Zhu, M. Bolte, H.-W. Lerner, M. C. Holthausen, M. Wagner, *Chem. Eur. J.* **2012**, *18*, 11284–11295.

[77] X. Liu, P. Wu, J. Li, C. Cui, *J. Org. Chem.* **2015**, *80*, 3737–3744.

[78] Z. Lu, H. Quanz, O. Burghaus, J. Hofmann, C. Logemann, S. Beeck, P. R. Schreiner, H. A. Wegner, *J. Am. Chem. Soc.* **2017**, *139*, 18488–18491.